
A HYBRID COOPERATIVE CO-EVOLUTION ALGORITHM FRAMEWORK FOR OPTIMISING POWER TAKE OFF AND PLACEMENTS OF WAVE ENERGY CONVERTERS

A PREPRINT

Mehdi Neshat

Optimization and Logistics Group
School of Computer Science
The University of Adelaide
Australia
mehdi.neshat@adelaide.edu.au

Bradley Alexander

Optimization and Logistics Group
School of Computer Science
The University of Adelaide
Australia
bradley.alexander@adelaide.edu.au

Markus Wagner

Optimization and Logistics Group
School of Computer Science
The University of Adelaide
Australia
markus.wagner@adelaide.edu.au

June 24, 2020

ABSTRACT

Wave energy technologies have the potential to play a significant role in the supply of renewable energy on a world scale. One of the most promising designs for wave energy converters (WECs) are fully submerged buoys. In this work we explore the optimisation of WEC arrays consisting of a three-tether buoy model called CETO. Such arrays can be optimised for total energy output by adjusting both the relative positions of buoys in farms and also the power-take-off (PTO) parameters for each buoy. The search space for these parameters is complex and multi-modal. Moreover, the evaluation of each parameter setting is computationally expensive – limiting the number of full model evaluations that can be made. To handle this problem, we propose a new hybrid cooperative co-evolution algorithm (HCCA). HCCA consists of a symmetric local search plus Nelder-Mead and a cooperative co-evolution algorithm (CC) with a backtracking strategy for optimising the positions and PTO settings of WECs, respectively. Moreover, a new adaptive scenario is proposed for tuning grey wolf optimiser (AGWO) hyper-parameter. AGWO participates notably with other applied optimisers in HCCA. For assessing the effectiveness of the proposed approach five popular Evolutionary Algorithms (EAs), four alternating optimisation methods and two modern hybrid ideas (LS-NM and SLS-NM-B) are carefully compared in four real wave situations (Adelaide, Tasmania, Sydney and

Perth) with two wave farm sizes (4 and 16). According to the experimental outcomes, the hybrid cooperative framework exhibits better performance in terms of both runtime and quality of obtained solutions.

Keywords Renewable energy · Cooperative Co-Evolution Algorithms · Adaptive Gray Wolf optimiser · Position optimisation · Power Take Off system · Wave Energy Converters.

1 Introduction

Renewable energy technologies make up an increasing proportion of new-build electricity generating worldwide [1]. Ocean wave energy is one very promising technology for contributing to growth in energy demand from renewable sources due to the high-energy densities of ocean environments, and high capacity factors wave energy converter (WEC) models [2]. It is envisaged that ocean wave energy could supply more than 70% of the worlds whole energy demand [3]; but the current WECs technologies are not fully developed due to the technical engineering challenges of harnessing ocean wave power in harsh ocean environments.

In this research, we apply a developed WEC simulator for evaluating the absorbed power of a wave farm consisting of CETO-6 model WEC converters [4]. CETO converters are spherical submerged three-tether buoys. These converters were first designed in 2007 by the Carnegie Clean Energy company [5]. The energy output of WEC's of this design is dependent on a number of factors including, the relative positions of WEC's in an array; the power-take-off (PTO) settings on each buoy's tethers; and the long-term sea conditions of the wave-farm site. In this work, we optimise both the position and PTO parameters of simulated wave farms consisting of both 4 and 16 buoys in 4 real wave environments.

Since computing the complex hydrodynamic interactions among converters is computationally costly, the evaluation of each WECs arrangement can take several minutes. Moreover, a combination of both search spaces WECs positions and PTOs creates a multimodal and large-scale optimisation problem. These challenges require the use of robust, low-cost global search heuristics customised to this problem domain. To date the best performing heuristics for this problem [6] have been hybrid optimisation methods that placed and refined buoys parameters one at a time.

In this paper, we propose a new hybrid cooperative co-evolution algorithm (HCCA) for optimizing WEC array positions and PTO parameters that builds on these previous approaches by: The main contributions of the HCCA are:

1. Developing the applied simulator for evaluating the PTOs configurations per each wave frequency, which is more close to the real sea states.
2. Extending the Grey Wolf Optimiser by a new adaptive mechanism (AGWO) for balancing exploration and exploitation.
3. Embedding the AGWO within a Cooperative Co-evolution method (SLPSO + SaNSDE) for optimizing the PTO configuration of the wave farm.

4. Employing a backtracking strategy to further optimise both position and PTO settings of the obtained array.

To evaluate this new algorithm, we compare HCCA to a comprehensive range of meta-heuristics for optimizing the total power output of a wave farm, including (1) five popular off-the-shelf EAs, (2) four cooperative optimisation ideas, and (3) three hybrid optimisation algorithms. We evaluate our using four real wave scenarios from the Southern coast of Australia (Perth, Sydney, Adelaide and Tasmania). Each scenario embeds a detailed model of a wave environment including time-integrated distributions of wave-heights, periods and directions. The experimental results show that HCCA is able to significantly outperform other optimisation approaches with regard to both convergence speed and total absorbed power output.

The remainder of the paper is organized as follows. We provide an overview of related work in Section 2, and introduce the mathematical model for the WECs being studied in Section 3. The optimisation setup and the proposed optimisation methods are described in Sections 4 and 5, respectively. In Section 6, the experimental results are presented. We conclude with a summary and outline potential future work.

2 Related Work

There have been a number of studies in optimising the power output a variety of WEC models. One initial study [7] optimised WEC positions for five buoys using both the Parabolic Intersection (PI) method and a GA. The study required a high number of function evaluations (37000). The wave environment modelled was highly simplified, with just one wave direction. A recent study by Ruiz et al. [8] employed another simple wave scenario to compare a custom GA, CMA-ES [9] and glow-worm optimisation (GSO) [10] for optimizing the position of the buoys in a discrete grid. The investigation found that while the convergence rate of CMA-ES is faster than of the other two methods, it could not overcome both the GA and GSO, in terms of total power production. In other recent WEC position optimisation research, Wu et al. [11] compared a 1+1EA and population-based evolutionary algorithm (CMA-ES) to optimise both 25 and 50 buoys using a simplified uni-directional irregular wave model. That paper revealed that the 1+1EA with a simple mutation operator is able to outperform CMA-ES. However, the performance achieved for both the 25 and 50-buoy layouts was low. Neshat et al. [12, 13, 14] characterized a more complicated wave scenario (seven wave directions and 50 wave frequencies) with the intra-buoy effects and employed this knowledge to make a customized, single-objective hybrid heuristic (local search + Nelder-Mead). However, the wave model still used an artificial wave scenario and the proposed method did not tune PTO parameters.

Another challenging aspect of maximizing the total power output of the wave farm is controlling the WECs' oscillations with respect to the incoming waves' frequency. This is because maximum efficiency will be achieved at resonance. However, maintaining a resonant condition can be challenging in real sea states with multiple different frequencies [15].

One way of achieving resonance is by configuring the power take-off (PTO) system of the WECs, either in online or offline settings. For then online setting, Ding et al. [16] implemented the maximum power point tracking (MPPT)

control method for optimising the damping rate (dPTO) of one converter (CETO 6). The MPPT is a type of online-optimisation based on the gradient-ascent algorithm. The outcomes reported a high efficiency of the MPPT damping controller compared with a fixed-damping system, but the performance of MPPT was not assessed for layouts with more than one buoy. In later work Abdelkhalik et al. [17] utilised the hidden genes genetic algorithm (HGGA) to tune PTO parameters. While the proposed optimiser boosted the total energy produced, HGGA's efficiency was not compared to other modern EAs.

Glass et al. [18] used a combination of a generic GA with an analytical multiple scattering method to optimise WECs parameters including buoy radius, draft, and converter damping. That work produced some 5 and 9-buoy layouts with constructive interactions in a simple (uni-directional) wave scenario. Silva et al. [19] compared the performance of a GA and COBYLA [20] (Constrained optimisation BY Linear Approximations) for maximizing the produced annual electrical output of one WEC with a U-shaped design inside an oscillating water column (UGEN) by adjusting PTO settings and the buoy's geometrical characteristics. The obtained results showed that COBYLA method converged to design with fewer evaluations. However, the GA produced a better solution overall, because COBYLA had converged to a local optimum. In another recent study, hybridization of a customized local search with a Nelder-Mead algorithm and a refinement strategy (SLS-NM-B) was introduced [6] for optimizing both arrangement and PTOs parameters of WECs model (CETO). While the optimisation results represented a considerable power improvement of SLS-NM-B compared with other popular EAs, the optimisation of the PTOs settings were optimised in unison.

3 Mathematical modelling for wave energy converters

3.1 Wave Resource

According to the latest real wave data set from Australian Wave Energy Atlas [21], different four wave sites on the southern coast of Australia are studied in this paper including Perth, Adelaide, Tasmania (southwest coast) and Sydney. Figure 1 shows the directional wave rose and wave scatter diagram of these four wave scenarios. It is observed that the applied wave regimes differ with regard to the directional distributions and cumulative energy. This diversity provides four various search spaces for evaluating the performance of the optimisation methods accurately. The applied model of the ocean wave is irregular directional waves embedding the Bretschneider spectrum [22].

3.2 Power Absorption Modelling

The applied WEC in this research is a symmetric, spherical and fully submerged buoy (minimum depth of 8m at the top of the buoy) with three-tethers. Each tether is attached to a mooring system installed on the seabed. The principal goal of the mooring system is to keep the floating structure in position within specific tolerances in both under normal load conditions and severe storm load conditions. The assumed optimal angle of each tether is 55 degrees [23]. The details of physical WECs characteristics, including submergence and ocean depth can be found in [12].

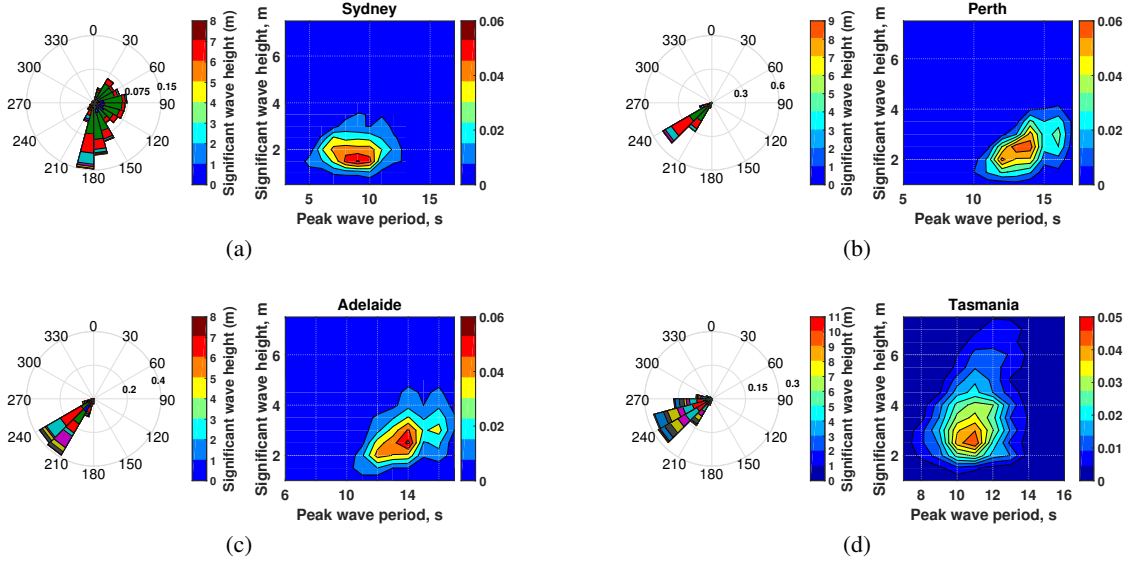


Figure 1: Scatter and wave rose diagrams for four wave energy sites in Australia: (a) Sydney, (b) Perth, (c) Adelaide and (d) Tasmania. These are: the directional wave rose (left) and wave scatter diagram (right).

For modelling the motion of a WEC in a frequency domain, three degrees (surge, sway and heave) of freedom are formulated based on linear wave theory. The applied hypotheses are the following:

$$\begin{aligned} \hat{F}_{exc,\Sigma} &= \left((M_{\Sigma} + A_{\sigma}(\omega))j\omega + B_{\sigma}(\omega) - \frac{K_{pto,\Sigma}}{\omega}j + D_{pto,\Sigma} \right) \ddot{X}_{\Sigma} \\ M &= mI_{3N} \\ K_{pto} &= K_{pto}I_{3N} \\ D_{pto} &= D_{pto}I_{3N} \end{aligned} \quad (1)$$

where F_{exc} is the frequency-dependent vector of excitation forces and M is known as a mass matrix (I_{3N} is the identity matrix with size $3N$). N is the number of WECs in the layout, and the constant 3 denotes the number of degrees of freedom. \ddot{X}_{Σ} is a vector of body acceleration in the surge, heave and sway directions. The matrices A and B define the hydrodynamic added-mass and radiation damping coefficients, respectively. The PTO mechanism is modelled on an oscillating spring. The K_{pto} and D_{pto} are, respectively, the stiffness of spring and damping PTO matrices. Each row of these matrices represents the settings for each buoy. For each buoy, there are 50 individual K_{pto} and D_{pto} parameter settings representing a tuned response to 50 different ocean wave frequencies. For modelling the hydrodynamic interaction between submerged buoys, a semi-analytical solution is given in [24].

For calculating the power output of an entire WEC array, Equation 2 computes the mean all WEC's power harnessed in a regular wave frequency environment: ω , amplitude, and wave angle β .

$$P_{\Sigma} = \frac{1}{4} \left(\hat{F}_{exc,\Sigma}^* \ddot{X}_{\Sigma} + \ddot{X}_{\Sigma}^* \hat{F}_{exc,\Sigma} \right) - \frac{1}{2} \ddot{X}_{\Sigma}^* B \ddot{X}_{\Sigma} \quad (2)$$

While we are able to calculate the total power of the wave farm in Equation 2, it is very computationally expensive, and the computational cost rises quadratically with the number of buoys. Note that, where there is constructive interaction between converters, the total power output can grow super-linearly with the number of buoys.

4 Optimisation Setup

The formulation of the optimisation problem to maximise the power output of a WEC array is:

$$P_{\Sigma}^* = \operatorname{argmax}_{X, Y, K_{pto}, D_{pto}} P_{\Sigma}(X, Y, K_{pto}, D_{pto})$$

where $P_{\Sigma}(X, Y, K_{pto}, D_{pto})$ shows the annual average power produced for given WEC locations and PTO settings in a 2-D coordinate system at x -positions: $X = [x_1, \dots, x_N]$, y -positions: $Y = [y_1, \dots, y_N]$ and Power Take-off configurations including $K_{pto} = \{[B_{k_1}^1, \dots, B_{k_{50}}^1], \dots, [B_{k_1}^N, \dots, B_{k_{50}}^N]\}$ and $D_{pto} = \{[B_{d_1}^1, \dots, B_{d_{50}}^1], \dots, [B_{d_1}^N, \dots, B_{d_{50}}^N]\}$. where B is the i th buoy here and $N \in \{4, 16\}$. it is assumed that all WECs are placed the same depth (5 metres) in ocean with the uniform depth of 30 metres.

Constraints In this work, there are three constraints, including constraints of farm boundaries, safe distance constraints between generators and constraints on PTOs variables. In terms of farm boundaries the positions of each buoy (x_i, y_i) in the wave farm is restricted to a square search space $S = [x_l, x_u] \times [y_l, y_u]$: where $x_l = y_l = 0$ and $x_u = y_u = \sqrt{N * 20000} m^2$. The minimum safety distance constraint, to allow for shipping egress, is set to 50 meters. The PTO constraints are on spring damping PTO coefficients of $d_l = 5 \times 10^4$, $d_u = 4 \times 10^5$ and $k_l = 1$, $k_u = 5.5 \times 10^5$. Where a candidate solution satisfies all the constraint functions, it is marked as a feasible layout. For handling both boundary constraints (position and PTOs), infeasible solutions are forced to the most adjacent feasible design. For the safety distance constraint, a steep penalty function is used:

$$\begin{aligned} Sum_{dist} = & \sum_{i=1}^{N-1} \sum_{j=i+1}^N (dist((x_i, y_i), (x_j, y_j)) - 50), \\ & \text{if } dist((x_i, y_i), (x_j, y_j)) < 50 \text{ else } 0 \end{aligned}$$

where sum_{dist} is the sum of violations of the safe distance between buoys. The Euclidean distance between both buoys i th and j th is denoted by $dist((x_i, y_i), (x_j, y_j))$. The penalty value to the total power absorbed of the wave farm is calculated by $(Sum_{dist} + 1)^{20}$. The penalty strongly encourages selecting feasible layouts during the optimisation process.

Computational Resources The optimisation approaches studies here are evaluated and compared for both 4 and 16 WEC arrays for four real wave scenarios. For comparing all proposed methods in a realistic design setting, a time budget criterion of three days is set for optimisation method trial on an HPC supercomputer with a 2.4GHz Intel 6148 processor running 12 processes in parallel with 128GB of RAM. On this platform, this mode of parallelisation usually accommodates more than ten times speedup. Note that the implementations of the proposed optimisation methods are

written to so as to exploit the parallel processing capabilities of the platform maximally. The software platform used for running the function evaluations and the optimisation algorithms is MATLAB R2018.

5 Optimisation Methods

In this research three different broad optimisation strategies are employed for maximizing the total absorbed power output of 4 and 16-buoy layouts in this research. The first approach applies search algorithms to all decision variables simultaneously. These variables include all the x and y buoy position and all of the PTO parameters. For 16 buoys this approach requires that over 1632 variables are optimised all at once. The second broad approach is to apply cooperative methods [25], which alternate between the optimisation of position and PTO parameters. The third strategy, used in [12, 6], places buoys sequentially (one-at-a-time). Under this strategy, the performance of three hybrid methods are evaluated and compared: $LS - NM$ [12], $SLS - NM - B$ [6], and a new hybrid cooperative EA (HCCA). The details of the algorithms evaluated for each strategy are summarised in Table 1.

5.1 Evolutionary Algorithms (All-at-once)

In these experiments, five popular EAs and a new adaptive variant of GWO are used to optimise all dimensions simultaneously. These EAs are: (1) covariance matrix adaptation evolutionary-strategy (CMA-ES) [9], (2) Differential Evolution (DE) [26], (3) Particle Swarm optimisation (PSO) [27], (4) Grey Wolf optimiser (GWO) [28] and (5) Nelder-Mead simplex direct search (NM) [29] is combined with a mutation operator (Nelder-Mead+Mutation). Furthermore, we introduce a new variant of GWO called the adaptive grey wolf optimiser (AGWO).

5.1.1 Adaptive Grey Wolf optimiser (AGWO)

The adaptive grey wolf optimiser is a new variant of the grey wolf optimiser that tunes hyper-parameter settings to improve performance in this search domain.

Overview of grey wolf optimiser (GWO) The GWO algorithm [28] is categorized as a bio-inspired stochastic method that mimics grey wolves hunting behaviours in a pack. In the population, there are four classes of responsibility: the alpha wolf is responsible for leading the pack members. Following positions are allocated to beta and delta wolves; these assist the alpha in decision making. The remainder of the pack is called omegas – these help sample the search space. GWO simulates some aspects of the hunting process including 1) searching for the prey (optimum), 2) encircling the prey, 3) hunting and 4) attacking the prey.

Encircling the prey

$$\vec{D} = |\vec{C} \cdot \vec{X}_p(t) - \vec{X}(t)| \quad (3)$$

Table 1: Review of the proposed framework methods employed in this paper. All approaches are restricted to the same computational budget constraint. parallelism can be categorised into two groups as per-individual or per-frequency according to the individuals number in the population.

Abbreviation	parallelizm	Description
All-at-once methods (Positions+PTO parameters)		
<i>CMA-ES</i>	per-individual	CMA-ES [9] all dimensions, $\mu = 4 + \text{int}(3 * \log(N_{var}))$, $\sigma = 0.3 * \text{Area}$
<i>DE</i>	per-individual	Differential evolution [26], $\mu = 50$, $F = 0.5$, $P_{cr} = 0.5$
<i>PSO</i>	per-individual	Particle Swarm optimisation [27]. with $\mu = 50$, $c_1 = 1.5$, $c_2 = 2$, $\omega = 1$ (linearly decreased)
<i>GWO</i>	per-individual	Grey Wolf Optimiser [28]. with $\mu = 50$, $\alpha = 2$ (linearly decreased to zero)
<i>AGWO</i>	per-individual	Adaptive Grey Wolf optimiser. Where $\mu = 50$, $\alpha = 2$ will be adaptively updated, $CN_m^{Max} = 0.3$, $CN_m^{Min} = 10^{-6}$, $C_f = 0.7$
<i>NM</i>	per-frequency	Nelder-Mead search [29] is run in all dimensions iteratively $MaxFunEvals = 100$
Cooperative Evolutionary Ideas		
$(2+2)CMA-ES+NM$	per-individual & frequency	CMA-ES ($\mu = \lambda = 2$) cooperates with Nelder-mead where the position optimisation is done by CMA-ES and Nelder-Mead adjusts the spring-damping coefficients of all buoys in the round robin fashion.
$(1+1)EA+NM$	per-frequency	Cooperative strategy of 1+1EA (all position dimensions, $P_{Mu} = \frac{1}{N}$) with linearly decreasing mutation step size (σ) per generation [30] at 100 iterations and then Nelder-Mead tries to optimise the PTO parameters in all dimensions.
<i>AGWO + NM</i>	per-individual & frequency	Adaptive GWO is in charge of optimizing the PTO settings of the buoys. Afterward, the position configuration of the best candidate is optimised by Nelder-Mead search. This cooperative process is repeated until the time budget runs out.
<i>CCOS</i>	per-individual	Cooperative Co-evolution of <i>SLPSO</i> and <i>SaNSDE</i> with Online Optimiser Selection [31]. Where $\mu = 50$, $\mathbb{A} = 2$, $\mathbb{C} = N \times 2$.
<i>SLPSO_{II}</i>	per-individual	Double Social Learning Particle Swarm optimisation, Setup for <i>SLPSO_{II}</i> from [31]. $\mu = 50$, $\mathbb{A} = 2$, $\mathbb{C} = N \times 2$
<i>SaNSDE_{II}</i>	per-individual	Double Self-adaptive Neighborhood Search Differential Evolution [31]. $\mu = 50$, F , P_{cr} and ρ are initialized at 0.5, but updated adaptively. $\mathbb{A} = 2$, $\mathbb{C} = N \times 2$
Hybrid optimisation methods (one-at-a-time)		
<i>LS + NM</i>	per-frequency	Repeated Local Sampling + Nelder Mead search [12] buoys are placed at normally distributed random offset ($\sigma = 100m$) from previous buoy and then ($MaxSam = 512$) the best candidate sample is chosen. Next, the PTO parameters of chosen sample are enhanced by Nelder-Mead search.
<i>SLS + NM + B</i>	per-frequency	Symmetric Local Sampling + Nelder-Mead + Backtracking [6]. The new buoy is locally placed by a symmetric search approach. Next, both configurations (positions and PTOs) are adjusted by Nelder-Mead iteratively. Finally, the backtracking strategy modifies least-well performing buoy's locations and PTOs.
<i>HCCA</i>	per-individual & frequency	Hybrid Cooperative Evolution Algorithm. SLS sets an initial location for each new buoy; Nelder-Mead optimises the buoy's position; then adjusts the PTOs. The process iterates until all buoys are placed. Backtracking is then applied to improves the positions and PTO settings for some buoys which have the lowest absorbed power.

$$\vec{X}(t+1) = \vec{X}_p(t) - \vec{A} \cdot \vec{D} \quad (4)$$

where \vec{D} describes the interval among the prey location \vec{X}_p and a member of the pack \vec{X} in the current iteration (t). Additionally, There are two coefficient vectors (\vec{A} and \vec{C}) for controlling the behaviours of the exploration and exploitation, which can be computed by Equations 5 and 7:

$$\vec{A} = 2 \cdot \vec{a} \cdot \vec{r}_1 - \vec{a} \rightarrow 0 \leq a \leq 2 \quad (5)$$

$$a = 2 - iter \cdot \left(\frac{2}{Max_{iter}} \right) \quad (6)$$

$$\vec{C} = 2 \cdot \vec{r}_2 \quad (7)$$

where a is linearly decreased from 2 to 0 during the optimisation process. And also two random variables r_1 and r_2 are generated between 0 and 1.

Hunting For having a successful exploration in the search space, the search agents (solutions) positions are updated based on the knowledge of three best-sampled candidates (alpha, beta and delta). This is because we assume a prior that a nearby optimum can be found among these best. The position update formulas (Equations 8, 9 and 10) are as follows.

$$\vec{X}(t+1) = \frac{\vec{X}_1 + \vec{X}_2 + \vec{X}_3}{3} \quad (8)$$

$$\begin{aligned} \vec{X}_1 &= \vec{X}_\alpha(t) - \vec{A}_1 \cdot \vec{D}_\alpha \\ \vec{X}_2 &= \vec{X}_\beta(t) - \vec{A}_2 \cdot \vec{D}_\beta \\ \vec{X}_3 &= \vec{X}_\delta(t) - \vec{A}_3 \cdot \vec{D}_\delta \end{aligned} \quad (9)$$

$$\begin{aligned} \vec{D}_\alpha &= |\vec{C}_1 \cdot \vec{X}_\alpha - \vec{X}| \\ \vec{D}_\beta &= |\vec{C}_2 \cdot \vec{X}_\beta - \vec{X}| \\ \vec{D}_\delta &= |\vec{C}_3 \cdot \vec{X}_\delta - \vec{X}| \end{aligned} \quad (10)$$

Attacking the prey (exploitation) The hunting manner is followed by attacking the prey and converging to the optimum positions. This can be achieved mathematically by reducing the a variable from 2 to 0 gradually. It is observed that when $|\vec{A}| < 1$ search agents are forced to attack the prey that is like a local search (exploitation process). Inversely, where $|\vec{A}| > 1$ leads to a global search (divergence) or exploration process.

Adaptive Grey Wolf optimiser (AGWO) One of the most critical parameters of GWO is \vec{A} because it can adjust both diversification ($|\vec{A}| > 1$) and intensification ($|\vec{A}| < 1$) of the search process. According to Equation 5, the vector

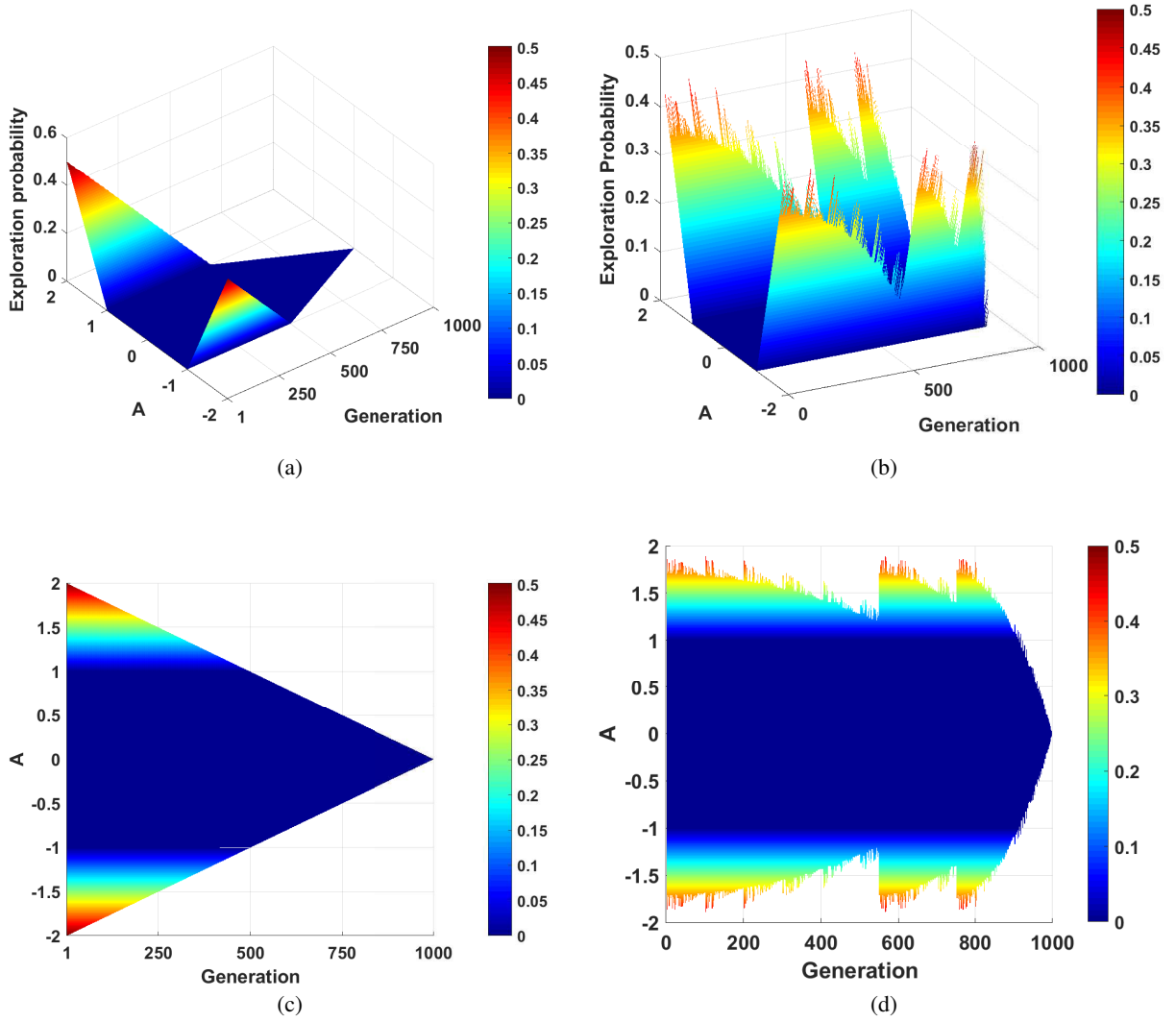


Figure 2: (a and c) The probability of original GWO exploration per generation (3D and 2D). (b and d) one example of the proposed adaptation mechanism for the control vector (a) . These figures show the AGWO exploration probability per generation (3D and 2D).

of \vec{A} values can be between $-a$ and a ($\vec{A} \in [-2a, 2a]$), where a is reduced linearly during the optimisation from 2 to 0. It means that the probability of exploration ($|\vec{A}| > 1$) at the initial iteration is 0.5 and will be linearly decreased until 0 in the middle of the search process. On the other hand, the exploitation probability in the first iteration is 0.5 that is similar to exploration probability (giving a balanced-heuristic setting at the start); however, the exploitation probability is gone up to 1 where half of the iterations are devoted ($iter = Max_{iter}/2$). Significantly, in the remaining iterations ($Max_{iter}/2$), exploitation probability is 1, but exploration probability is 0 without any change. This issue is one reason why GWO is faced with premature convergence in some cases. Figure 2 (a and c) show this unbalanced search behavior. To overcome this shortcoming, a number of different mechanisms have been suggested.

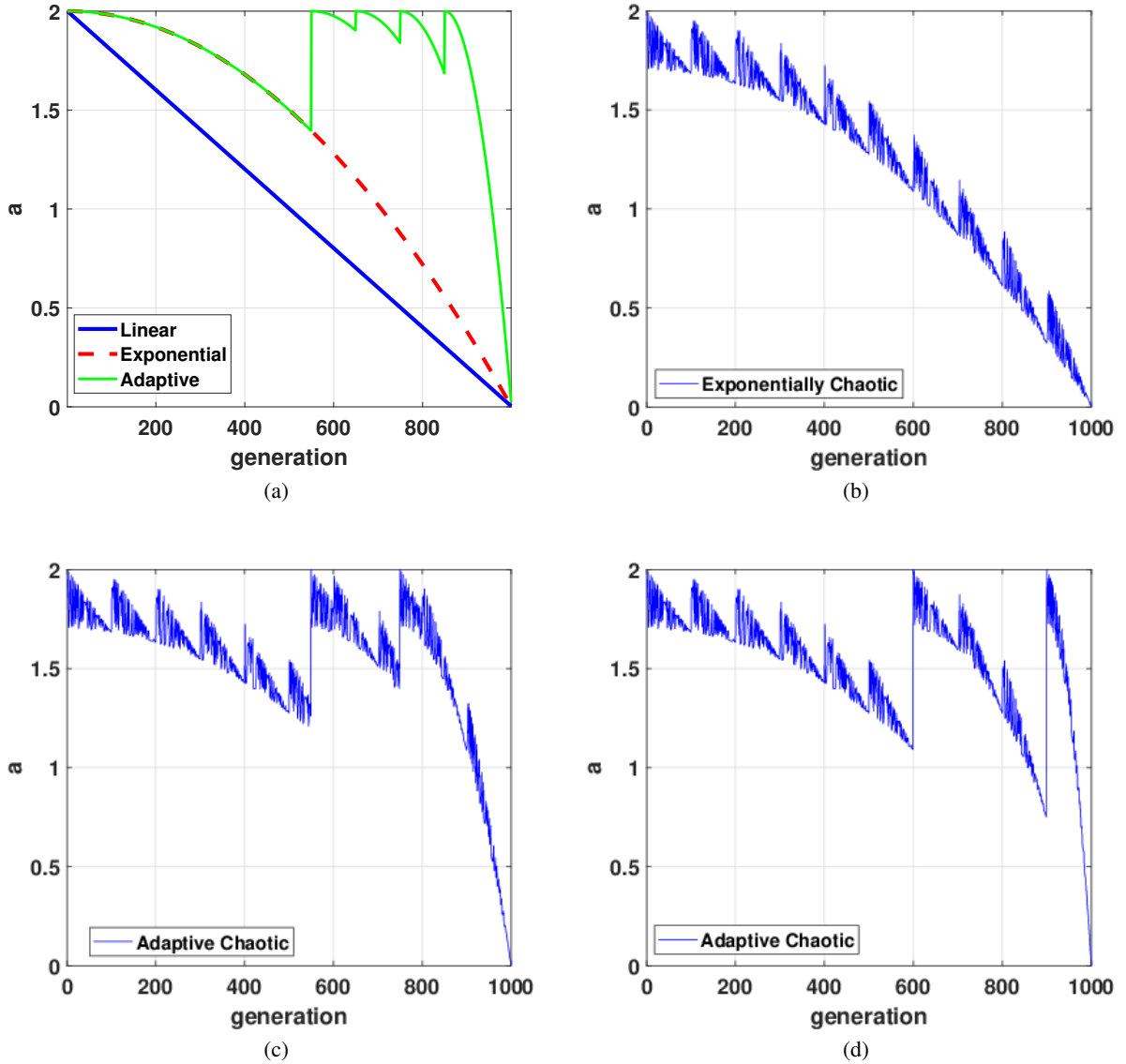


Figure 3: (a) the original strategy of control variable a decreases linearly[28](blue line) and in [32] it polynomially decreases (red line). This decay process can be adapted based on the optimisation process achievements (green line) which is introduced by this research. (b) shows a combination of polynomial and chaotic behavior of the control variable. This chaotic behavior is normalized and periodic. Graphs (c) and (d) show decay plots that combine both adaptive and chaotic decay. The use of adaptation and its combination with chaotic decay is new to the AGWO algorithm described here.

Mittal et al. [32] proposed an improved version for updating \bar{a} in (mGWO) which decayed more slowly to improve exploration. Figure 3(a) represents this slower decay function. However, in this static mechanism after 70% of the iterations, the value of a has still decayed below 1. A similar modification was introduced by Long et al. [33] in their Improved Grey Wolf optimiser (IGWO). More recently, Saxena et al. [34] scaled the decay function using a β -chaotic sequence to allow for faster oscillation between exploration and exploitation phases during the parameter decay process.

In previous research, various approaches were recommended for adjusting the a parameter, but these ideas did not pay attention to the GWO performance during the optimisation. In this paper, we propose an adaptive mechanism for updating the control variable a of GWO (AGWO). In this way, the optimisation performance is observed, and after a pre-determined period of ρ iterations, where the best-found solution does not overcome the alpha particle, the control parameter should be incremented back to 2. Moreover, a chaotic distribution is implanted with mapping by a normalize function for obtaining a great balance between exploration and exploitation. The main AGWO contributions can be seen in the following:

1. Generating and combining a chaotic sequence with the control parameter (a) in each iteration. For achieving the best performance, ten various chaotic maps are applied and compared. Table 3 shows the applied these chaotic maps in the adaptive idea.
2. Using the normalization function periodically for distributing the chaotic sequence between upper and lower bias. The mathematical formulation of the function can be represented by Equation 11.

$$N_{m_{iter}} = CN_m^{Max} - \left(\frac{CN_m^{Max} - CN_m^{Min}}{Max_{iter_N}} \right) \times iter_N \quad (11)$$

Where the maximum and minimum values of the normalization function are $CN_m^{Max} = 0.3$ and $CN_m^{Min} = 10^{-6}$, respectively. And also Max_{iter_N} is the maximum iterations in each period. Therefore, the normalized chaotic values (CC_{iter}) can be produced by Equation 12:

$$CC_{iter} = N_{m_{iter}} * Cf \quad (12)$$

Where Cf is generated by the applied chaotic map. One example of the adaptive chaotic mechanism is presented in Figure 2(b,d). The generated value of the chaotic sequence is embedded in control vector \vec{a} and is presented in following equation:

$$a = (2 - CN_m^{Max}) - (iter_c^2 \times \frac{2 - CN_m^{Max}}{Max_{iter_c}^2}) + CC_{iter} \quad (13)$$

3. Introducing an adaptive mechanism for updating the control vector when the optimisation results are not satisfied for ρ iterations. When search stagnates in this way, the control vector is reset to 2, and then the decay slope of the control vector is adjusted to a sharper gradient. This results in a switch from exploitation ($|\vec{a}| < 1$) to exploration when search stagnates.

Figure 3 demonstrates various mechanisms for updating the control vector include linear and polynomial ideas (a), and three samples of the new adaptive chaotic method (b,c and d).

To sum up, AGWO is a combination of the ideas which consist of 1) an adaptive updating mechanism for tuning the \vec{a} that depending on current search performance. Consequently, this feature of AGWO facilitates a balance between exploration and exploitation processes throughout the entire search. 2) a chaotic sequence coefficient which scales

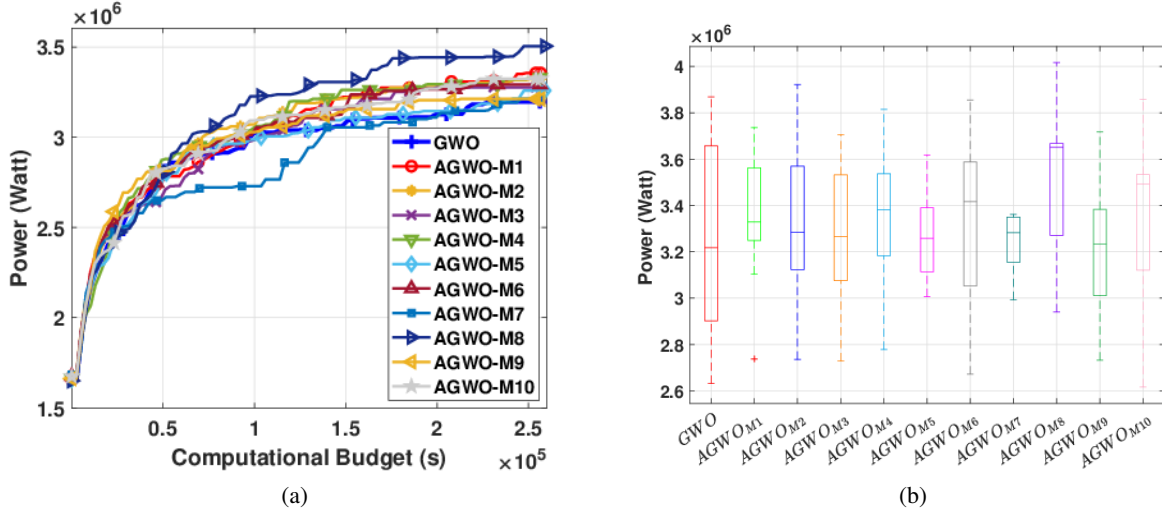


Figure 4: The convergence (a) and quality (b) comparison of the 10 different chaotic maps (M1-M10 Table 3) combined with AGWO performance for 16-buoy layouts in Perth wave model. (10 independent runs for each configuration.)

the normalization function and further helps prevent the premature convergence (avoidance of local minima). The pseudo-code of the AGWO is presented in Algorithm 1.

In order to measure and test the impact of various chaotic maps on the AGWO performance, a set of well-known chaotic maps [35, 36, 37, 38] are applied. Table 3 shows the details of these maps (M_1, M_2, \dots, M_{10}) and the summaries of AGWO parameters settings are listed in Table 1. The parallelization of search is done per individual, and a 16-buoy layout size of the Perth wave model is selected as a case study. The results of Figure 4 and Table 2 are reported over ten independent runs. It can be seen that applying the chaotic maps with the adaptive strategy results in improved performance for GWO. In comparison to GWO results, the best performance is produced by the $M_8(Singer)$ map with better convergence speed and the average total power outputs improved by 3.83% and 7.95%, respectively. Based on this performance, we use $M_8(Singer)$ for the chaotic map in the following experiments.

5.2 Cooperative optimisation methods

Wave farm parameter (Position+PTO settings) optimisation has a very high dimensionality which makes it a challenging search problem. One option for dealing with this issue is to divide the decision variables into two subsets: WEC positions and PTO settings. This decreases the problem dimension and provides a more homogeneous search space. Four cooperative optimisation techniques are proposed and compared including a new combination of AGWO and the Nelder-Mead, hybrid of (2+2)CMAES and Nelder-Mead [6], and a combination of a 1+1EA and Nelder-Mead [6], and, finally, the CCOS algorithm introduced in [31]. Details of these algorithms are as follows:

5.2.1 AGWO + Nelder-Mead

(AGWO-NM) As GWO is designed as an unconstrained meta-heuristic idea, it is not able to handle the constraint of WECs distances (safe distance) easily. However, GWO can be a fast and effective unconstrained optimisation method.

Algorithm 1 Adaptive Grey Wolf optimiser (AGWO)

```

1: procedure AGWO
2:    $size = \sqrt{N * 20000}$  ▷ Farm size
3:    $Np = 50$  ▷ Population size
4:    $\mathbf{S} = \{ \langle x_1, y_1, B_{k_1}^1, \dots, B_{k_{50}}^1, B_{d_1}^1, \dots, B_{d_{50}}^1 \rangle, \dots$ 
5:    $\langle x_{Np}, y_{Np}, B_{k_1}^{Np}, \dots, B_{k_{50}}^{Np}, B_{d_1}^{Np}, \dots, B_{d_{50}}^{Np} \rangle \}$  ▷ Initial Population
6:    $energy = Eval([S_1, S_2, \dots, S_{Np}])$  ▷ Evaluate Layouts
7:   Initialize parameters  $a, A, C, CN_m^{Max}, CN_m^{Min}, \rho$  and  $Max_{iter_N}$ 
8:    $X_\alpha = \text{The best layout from } \langle S_1, \dots, S_{Np} \rangle$  ▷ Find three best layouts
9:    $X_\beta = \text{The second best layout from } \langle S_1, \dots, S_{Np-1} \rangle$ 
10:   $X_\delta = \text{The third best layout from } \langle S_1, \dots, S_{Np-2} \rangle$ 
11:  while stillTime() do
12:    for  $i$  in  $[1, \dots, Np]$  do
13:      Update  $S_i$  by Equation 8
14:      if  $S_i$  is not feasible then
15:         $S_i = Repair(S_i)$  ▷ replacing by nearby feasible solution
16:      end if
17:    end for
18:     $energy = Eval([S_1, S_2, \dots, S_{Np}])$  ▷ Evaluate Layouts
19:     $BestEnergy_{iter} = Max(energy)$ 
20:    if  $rem(iter, \rho) = 0$  &  $BestEnergy_{iter} < f(X_\alpha)$  then
21:       $a = 2, iter_N = 1$  and  $iter_c = 1$  ▷ Reset control variables
22:    else ▷ Reset iteration of normalization and chaotic sequence
23:      Update  $N_{m_{iter}}, CC_{iter}$  and  $Cf$  by Equation 11,12
24:      Update  $a, A$  and  $C$  by Equation 13,7,6
25:    end if
26:    Update  $X_\alpha, X_\beta$  and  $X_\delta$ 
27:  end while
28:  return  $S, energy$  ▷ Final Layout
29: end procedure

```

In this way, a combination of AGWO and Nelder-Mead is proposed that AGWO adjusts the PTO configurations of WECs to achieve the highest power output and then NM is used for optimizing the arrangement of buoys. This optimisation process is run iteratively using the same computational budget until the runtime (three days) runs out.

5.2.2 Cooperative Co-evolution with Online optimiser Selection: CCOS

The Cooperative Co-evolution with an online mechanism for selecting the suitable optimiser (CCOS) introduced by Sun et al. [31]. The CCOS consists of two general parts: decomposition and optimisation. In the first stage, a robust recursive algorithm [39] is used to group parameters into subsets based on how they correlated during optimisation. These subsets are recursively decomposed according to the strength of parameters interactions. The algorithm is able to decompose an n -dimensional problem using $\mathcal{O}(n \log n)$ steps. During the optimisation phase, two state-of-the-art adaptive optimisers are employed; the social learning particle swarm optimiser (SLPSO [40]), and self-adaptive differential evolution with neighbourhood search (SaNSDE [41]). The main contributions of SaNSDE are 1) incorporating the search biases of distributions, Cauchy and Gaussian operators. SaNSDE takes into account the trade-off between small and large mutation step sizes; 2) all control parameters of SaNSDE are self-adapted based on statistical performance tracking during the optimisation process. Moreover, to assess the CCOS algorithm (SLPSO+SaNSDE) thoroughly, we compared CCOS's performance against the performances of a double SLPSO ($SLPSO_{II}$) and SaNSDE ($SaNSDE_{II}$). This evaluation helps isolate the impact of using these optimisers cooperatively.

5.3 Hybrid optimisation algorithms

In the earlier work, a practical WECs optimisation idea was developed [12] called Local Search + Nelder Mead (LS-NM); that showed using a local sampling by a normal distribution in the previous buoy’s neighbourhood (outside of the safe distance) combined with greedy selection could produce high-performing layouts. Such one-at-a-time placement is a fast optimisation strategy. However, tuning the position of the placed buoys required a considerable computational budget. This work also did not consider other WEC optimisation parameters such as PTO settings.

More recently [6] proposed an improved heuristic (SLS-NM-B) for placing the new WEC one-at-a-time and tuning PTOs settings. As local sampling in LS-NM is done without strong regard to useful priors of direction and distance, a repaired step is needed to modify the current position. SLS-NM-B represented a symmetric local search with the deterministic directions and bounded search space. Moreover, a backtracking strategy was introduced for improving the WEC parameters including both position and PTO settings (with the latter being tuned in unison for each buoy). Nevertheless, SLS-NM-B was not designed to handle the high dimensional search problem that arises when all PTO frequency response settings are allowed to move independently. This is because the Nelder-Mead optimiser that is applied for tuning the PTO parameters converges extremely slowly in the high-dimensional search space [42]. Moreover, it has not been proven that the PTO parameter space in this problem is uni-modal and so the downhill search heuristics such as Nelder-Mead may not be suitable for global optimisation.

5.3.1 Hybrid Cooperative Co-evolution algorithm (HCCA)

One of the most effective strategies for solving the large-scale optimisation problems is Cooperative Co-evolution (CC) framework [43]. In CC, the general idea is dividing the decision variables into some components (decomposition) and employing one or more optimisers in a round-robin fashion (in biased or unbiased mode) for optimizing the sub-problems. In this paper, as a combination of WECs placements and PTOs settings forms a large number of decision variables ($N \times 102$) with a complex search space, we propose a new hybrid Cooperative Co-evolution (HCCA) method. The steps of the proposed hybrid algorithm are described in more details as follows.

Decomposition: In the decomposition phase, we apply a knowledge-based approach according to the significant WECs hydrodynamic rule [44]. The rule is that both PTO parameters (damping coefficient ($dPTO$) and spring stiffness ($kPTO$)) of each converter should be optimised together. Therefore, the problem is decomposed into two sub-problems for each WEC, including PTO settings ($\langle B_{k_1}^i, \dots, B_{k_{50}}^i, B_{d_1}^i, \dots, B_{d_{50}}^i \rangle, 100D$) and position ($\langle x_i, y_i \rangle, 2D$).

optimisation: The HCCA optimisation phase is comprised of optimisation phases for the two-parameter groups listed above. For the buoy position parameter-group, the hybrid systematic neighbourhood search from(SLS-NM) [6] is applied by first uniformly sampling in search sectors whose boundaries are informed by an initial 2-buoy power landscape analysis. After this, a Nelder-Mead search is used to improve the best-sampled positions.

Algorithm 2 HCCA

```

1: procedure HYBRID COOPERATIVE CO-EVOLUTION ALGORITHM
2: Initialization
3:    $size = \sqrt{N * 20000}$  ▷ Farm size and  $N$  is buoy number
4:    $\mathbb{A}_{ii} = \{1 \leq ii \leq |\mathbb{A}|\}$  ▷ candidate optimisers
5:    $angle = \{0, 45, 90, \dots, 315\}$  ▷ symmetric samples angle
6:    $iters = Size(|angle|)$  ▷ Number of symmetric samples
7:    $\mathbb{S} = \{\langle x_1, y_1, B_{k_1}^1, \dots, B_{k_{50}}^1, B_{d_1}^1, \dots, B_{d_{50}}^1 \rangle, \dots$ 
8:    $\dots, \langle x_N, y_N, B_{k_1}^N, \dots, B_{k_{50}}^N, B_{d_1}^N, \dots, B_{d_{50}}^N \rangle\}$  ▷ Positions&PTOs
9:    $\langle \mathbb{S}_1, \mathbb{S}_2, \dots, \mathbb{S}_N \rangle = Decompose(\mathbb{S})$  ▷ Decomposing  $\mathbb{S}$  per buoy
10:   $\left\{ \begin{array}{l} \mathbb{S}_1 = \{\langle x_1, y_1 \rangle, \langle B_{k_1}^1, \dots, B_{k_{50}}^1, B_{d_1}^1, \dots, B_{d_{50}}^1 \rangle\} = \perp \\ \mathbb{S}_2 = \{\langle x_2, y_2 \rangle, \langle B_{k_1}^2, \dots, B_{k_{50}}^2, B_{d_1}^2, \dots, B_{d_{50}}^2 \rangle\} = \perp \\ \dots \\ \mathbb{S}_N = \{\langle x_N, y_N \rangle, \langle B_{k_1}^N, \dots, B_{k_{50}}^N, B_{d_1}^N, \dots, B_{d_{50}}^N \rangle\} = \perp \end{array} \right.$ 
11:   $U_{\mathbb{A}_{ii}, \mathbb{S}_i} = 0$  ▷ Initialize the accumulated contributions of optimisers
12:   $\mathbb{S}_1 = \{\langle size, 0 \rangle, \langle r_1 \times Max_k, r_2 \times Max_d \rangle\}$  ▷ initialize first buoy
13:  if  $i = 1$  then ▷ optimise first buoy PTOs by the optimisers
14:    for  $ii$  in  $|\mathbb{A}|$  do ▷ Calculate contribution
15:       $\langle I_{(\mathbb{A}_{ii}, \mathbb{S}_i)}, Energy \rangle = optimise(\mathbb{S}_{iPTOs}, \mathbb{A}_{ii})$ 
16:       $U_{(\mathbb{A}_{ii}, \mathbb{S}_i)} = (\hat{U}_{(\mathbb{A}_{ii}, \mathbb{S}_i)} + I_{(\mathbb{A}_{ii}, \mathbb{S}_i)}) / 2$  ▷ Accumulate contribution
17:    end for
18:     $\mathbb{S}_{i+1PTOs} = \mathbb{S}_{iPTOs}$ 
19:  end if
20:   $BestIndex = Max(U_{(\mathbb{A}_{ii}, \mathbb{S}_i)} \rightarrow 1 \leq ii \leq |\mathbb{A}|)$ 
21:  for  $i$  in  $[2, \dots, N]$  do  $bestEnergy = 0;$ 
22:    for  $j$  in  $[1, \dots, iters]$  do
23:       $\langle Sample_j, energy_j \rangle = SymmetricSample(angle_j, \mathbb{S}_{(i-1)})$ 
24:      if  $Sample_j$  is feasible &  $energy_j > bestEnergy$  then ▷ Temporary buoy position
25:         $tPos = Sample_j$ 
26:         $bestEnergy = energy_j$ 
27:         $bestAngle = j$ 
28:      end if
29:    end for
30:     $\langle Es_1, Es_2 \rangle = SymmetricSample(bestAngle \pm 15, \mathbb{S}_{(i-1)})$ 
31:     $\langle \mathbb{S}_{(i)}, energy \rangle = FindbestS(tPos, Es_1, Es_2)$ 
32:    PTO settings Optimisation
33:     $\langle I_{(\mathbb{A}_{BestIndex}, \mathbb{S}_i)}, Energy \rangle = optimise(\mathbb{S}_{iPTOs}, \mathbb{A}_{BestIndex})$ 
34:     $U_{(\mathbb{A}_{BestIndex}, \mathbb{S}_i)} = (\hat{U}_{(\mathbb{A}_{BestIndex}, \mathbb{S}_i)} + I_{(\mathbb{A}_{BestIndex}, \mathbb{S}_i)}) / 2$ 
35:     $BestIndex = Max(U_{(\mathbb{A}_{ii}, \mathbb{S}_i)} \rightarrow 1 \leq ii \leq |\mathbb{A}|)$ 
36:     $\mathbb{S}_{i+1PTOs} = \mathbb{S}_{iPTOs}$ 
37:    Position Optimisation
38:     $\langle \mathbb{S}_i, Energy \rangle = Nelder-Mead(\mathbb{S}_{iPosition})$ 
39:  end for ▷ Call BackTracking procedure
40:
41:   $\langle \mathbb{S}, Energy \rangle = BackTracking(\mathbb{S}, \mathbb{A}_{BestIndex})$ 
42: end procedure

```

In the second group of the optimisation, we propose a Cooperative Co-evolution idea for adjusting the PTOs settings that is a large-scale optimisation problem ($N \times 100$). This CC framework is composed of three modern and efficient optimisers, SLPSO [40], SaNSDE [41] and a new proposed adaptive grey wolf optimiser (AGWO). The SLPSO is a competitive optimiser [31] for working in the context of CC because 1) it is computationally efficient, 2) needs no complicated fine-tuning of the control parameters, 3) has a high exploitation ability and convergence speed and 4) has worked well solving dimensional optimisation problems. However, converging to a local optimum can be a problem encountered with SLPSO. Consequently, for developing the CC framework, combine this with another optimiser with a high capability of the exploration. The SaNSDE optimiser has considerable capacity for exploration and has been broadly applied in the CC domain [45]. The third optimiser used here in CC framework is AGWO which is the new GWO variant described earlier. During optimisation these three optimisers share the same population and solve the components collaboratively. The Pseudo-code of the proposed HCCA algorithm for solving the WEC optimisation problem is shown in Algorithm 2.

Backtracking: After initial placement and PTO optimisation by the CC framework above a customized backtracking optimisation algorithm (BOA) The BOA refines both buoy positions and PTO parameters. For positions, the buoys with the lowest power output are selected and then NM is applied for optimizing the positions one at a time. For PTO parameters an optimiser is selected the best prior optimiser performance during the first search phase. The selected optimiser is then used to tune all of PTOs settings of the layout in all-at-once global search. The pseudo-code of the backtracking approach is given in Algorithm 3.

Figure 5 provides a graphical view of the proposed hybrid optimisation framework. In the first cycle, after placing the first buoy in a predefined location (recommended by [6]), the three optimisers (\mathbb{A}) are employed to resolve PTOs settings ($\mathbb{S}_{j_{PTOs}}$). Each optimiser is given the same computational budget. Next, each optimiser's contribution is computed as a fitness improvement ($I_{(\mathbb{A}_i, \mathbb{S}_j)}$):

$$I_{(\mathbb{A}_i, \mathbb{S}_{j_{PTOs}})} = \frac{f(\dot{\mathbb{S}}_{j_{PTOs}}) - f(\mathbb{S}_{j_{PTOs}})}{f(\dot{\mathbb{S}}_{j_{PTOs}})} \quad i \in \{1 \leq i \leq |\mathbb{A}|\}, \quad j \in \{1 \leq j \leq N\} \quad (14)$$

where $f(\dot{\mathbb{S}}_{j_{PTOs}})$ and $f(\mathbb{S}_{j_{PTOs}})$ show the power of the layout obtained before and after employing i^{th} optimiser in one cycle. The fitness improvement is a measure of the optimiser's ability to adjust the j^{th} buoys PTOs settings. For updating the fitness improvement for each optimiser during the whole optimisation process, an accumulated contribution variable is used [31]. This performance tracking is encoded in Equation 15.

$$U_{(\mathbb{A}_i, \mathbb{S}_{j_{PTOs}})} = \frac{\dot{U}_{(\mathbb{A}_i, \mathbb{S}_{j_{PTOs}})} + I_{(\mathbb{A}_i, \mathbb{S}_{j_{PTOs}})}}{2} \quad (15)$$

where $\dot{U}_{(\mathbb{A}_i, \mathbb{S}_{j_{PTOs}})}$ tracks each optimiser's (\mathbb{A}_i) accumulated contributions. In the first cycle, the $\dot{U}_{(\mathbb{A}_i, \mathbb{S}_{j_{PTOs}})}$ is initialized to 0. The accumulated contribution $U_{(\mathbb{A}_i, \mathbb{S}_{j_{PTOs}})}$ is the average of all fitness profits for each optimiser from previous cycles. In the next iteration, the best optimiser accumulated contribution

Hybrid Cooperative Co-evolution Algorithm

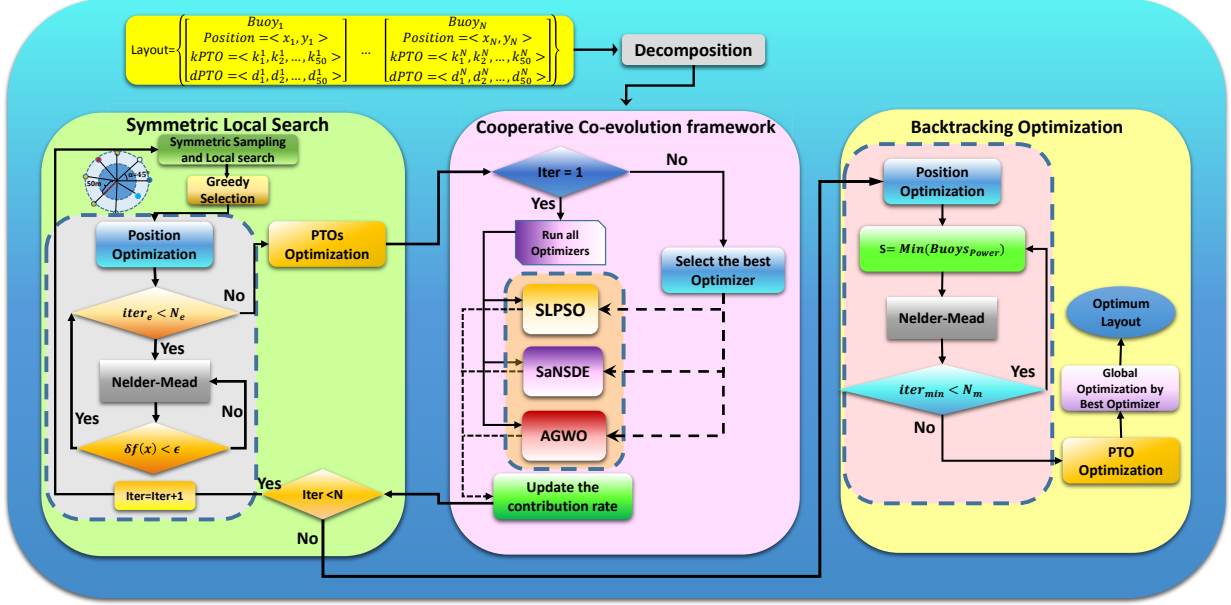


Figure 5: Outline of the Hybrid Cooperative Co-evolution Algorithm (HCCA). N , N_e and N_m are the maximum buoy number in the layout, the maximum evaluation number of Nelder-Mead and the buoy numbers for refining their positions. ϵ is the Nelder-Mead function tolerance and stopping criterion.

($BestIndex = Max(U_{(A_i, S_{jPTOs})} \rightarrow 1 \leq i \leq |A|)$) will be selected for optimizing the PTOs settings of the next placed generator. Figure 6 presents the average contribution of each applied optimiser for tuning the PTOs configuration of 16-buoy layouts in the Perth wave model. It can be seen that after the initial cycle the percentage contribution of SLPSO and SaNSDE is more than AGWO; however, for the last generations, AGWO's contribution is larger than that of the other optimisers.

After placing and optimizing the first buoy attributes, For each following buoy placement, eight symmetric local samples (SLS-NM) are done in different angles with the same resolution at 45° . However, the samples distances from the previously placed buoy are uniformly based on the bounded radial distance of between 50 (safe distance) and $50 + R'$. The best solution is chosen among all created symmetric samples. The infeasible solutions are ignored, and if all symmetric samples are infeasible, a feasible solution is performed by uniform random sampling. Also, then Nelder-Mead practices optimizing the position of the last-placed buoy. These both position and PTOs settings optimisation processes continue until the last buoy of the wave farm is placed and optimised. In the following, the backtracking strategy is run until the computational budget is depleted.

6 Experiments

This section starts with a small landscape study of the PTO parameter settings for a single buoy for the Perth wave scenario followed by a sensitivity analysis of the best-obtained 16-buoy layouts position. After that, we present the

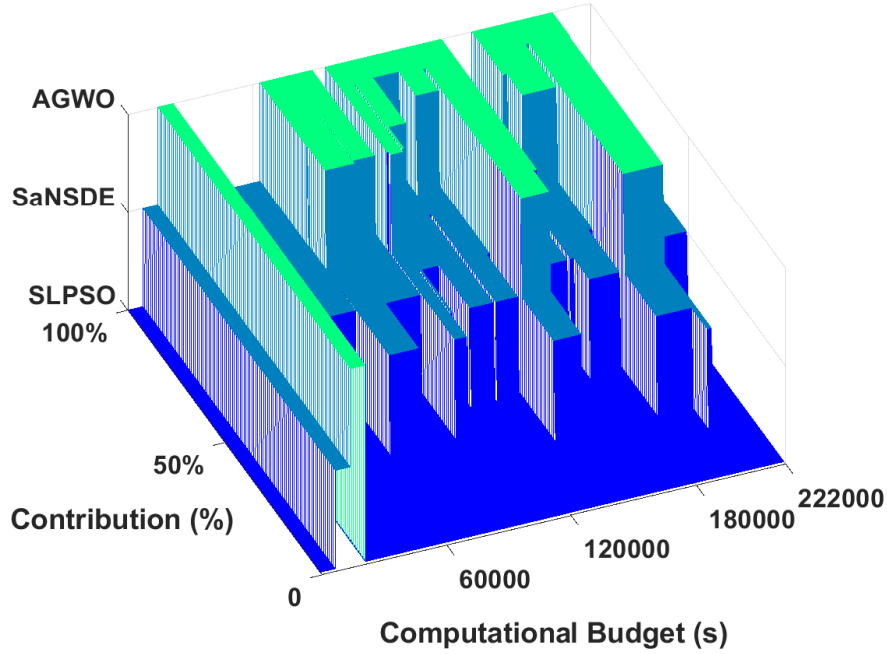


Figure 6: The contribution percentage of HCCA optimisers (SLPSO, SaNSDE and AGWO) in the optimisation process when used to optimise the PTOs settings of 16-buoy layout in Perth wave Scenario.

Perth wave scenario (16-buoy)											
	GWO	$AGWO_{M_1}$	$AGWO_{M_2}$	$AGWO_{M_3}$	$AGWO_{M_4}$	$AGWO_{M_5}$	$AGWO_{M_6}$	$AGWO_{M_7}$	$AGWO_{M_8}$	$AGWO_{M_9}$	$AGWO_{M_{10}}$
Max	3869188	3736690	3921497	3704994	3815293	3618343	3855858	3361619	4017436	3717341	3858006
Min	2631382	2737420	2735143	2728993	2778637	3006472	2671713	2993289	2940571	2731852	2616268
Mean	3258013	3361803	3324371	3276833	3335201	3258500	3324113	3216207	3517184	3212008	3331664
Median	3218467	3328703	3285224	3265160	3382717	3235225	3417449	3230982	3664481	3234115	3493016
STD	428448	278820	328343	280856	288771	199893	385533	142654	322678	305389	350371

Table 2: Results of 10 chaotic maps on the case study of Perth wave model on AGWO

optimisation outcomes of the experiments comparing the effectiveness of the proposed algorithms explained above applied to WEC positions and PTOs settings under four real wave scenarios. In order to characterise the scalability of the frameworks, we apply them to both the 4-buoy ($= 4 \times 102D$), and 16-buoy ($= 16 \times 102D$) have been evaluated in the experiments. Finally, the algorithm convergence rates and the quality of the obtained solutions are also compared.

6.1 Landscape analysis

6.1.1 PTOs settings analysis

In recent work [6], the impact of PTO parameter optimisation where these control parameters are kept the same for all wave frequencies for each buoy, was investigated and presented. This work found that tuning the PTOs parameters can be effective in optimising the total absorbed power of WECs (CETO model) in both Perth and Sydney wave climates by 4.48% and 2.42% , respectively. Figure 8 illustrates the PTO power landscape of one buoy with a simple grid search for tuning the damping-spring variables, where settings are kept the same for all wave frequencies.

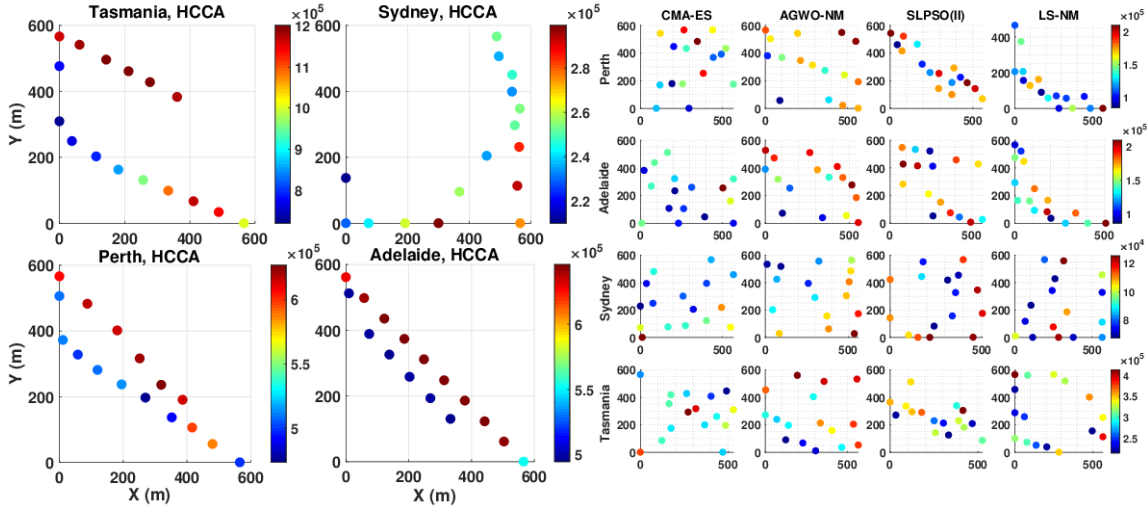


Figure 7: The best-found 16-buoy layouts arrangement of the four real wave scenarios based on Table 5.

NO.	Name	Chaotic Map	Range
1	Chebyshev	$x_{i+1} = \cos(\text{icos}^{-1}(x_i))$	(-1,1)
2	Circle	$x_{i+1} = \text{mod}(x_i + b - (\frac{a}{2\pi})\sin(2\pi x_i), 1), a = 0.5 \text{ and } b = 0.2$	(0,1)
3	Gauss/mouse	$x_{i+1} = \begin{cases} 1 & x_i = 0 \\ \frac{1}{\text{mod}(x_i, 1)} & \text{otherwise} \end{cases}$	(0,1)
4	Iterative	$x_{i+1} = \sin(\frac{a\pi}{x_i}), a = 0.7$	(-1,1)
5	Logistic	$x_{i+1} = ax_i(1 - x_i), a = 4$	(0,1)
6	Piecewise	$x_{i+1} = \begin{cases} \frac{x_i}{P} & 0 \leq x_i < P \\ \frac{x_i - P}{0.5 - P} & P \leq x_i < 0.5 \\ \frac{1 - P - x_i}{0.5 - P} & 0.5 \leq x_i < 1 - P, P = 0.4 \\ \frac{1 - x_i}{P} & 1 - P \leq x_i < 1 \end{cases}$	(0,1)
7	Sine	$x_{i+1} = \frac{a}{4}\sin(\pi x_i), a = 4$	(0,1)
8	Singer	$x_{i+1} = \mu(7.86x_i - 23.31x_i^2 + 28.75x_i^3 - 13.302875x_i^4), \mu = 1.07$	(0,1)
9	Sinusoidal	$x_{i+1} = ax_i^2\sin(\pi x_i), a = 2.3$	(0,1)
10	Tent	$x_{i+1} = \begin{cases} \frac{x_i}{0.7} & x_i < 0.7 \\ \frac{10}{3}(1 - x_i) & x_i \geq 0.7 \end{cases}$	(0,1)

Table 3: The applied chaotic maps from [36].

However, in the real sea states, WECs control parameters (PTOs) should be tuned for each wave frequency. By tuning these parameters independently for each buoy, it is possible to extract more power. We allow the PTO settings for all frequencies to be used for all proposed optimisation methods in this paper. For visualising the potential impact of PTO parameter optimisation for each wave frequency, a simplified experiment is done. Since the dimensionality of this problem is high (2×50 for a single buoy), we divide the 50 frequencies into 10 groups. Each group includes five sequential frequencies, and we constrain them to have the same PTOs parameters. The 45 wave frequencies in each group are assigned by the manufacturer’s PTOs defaults ($k = 407510$ and $d = 97412$) [12]. Figure 9 shows the modified PTOs optimisation power landscape of 10 groups for one buoy in Perth wave model, and for mixing all ten surfaces at one 3D figure, a normalised version of all landscapes is plotted (left figure) as a multi-layer 3D plot. We

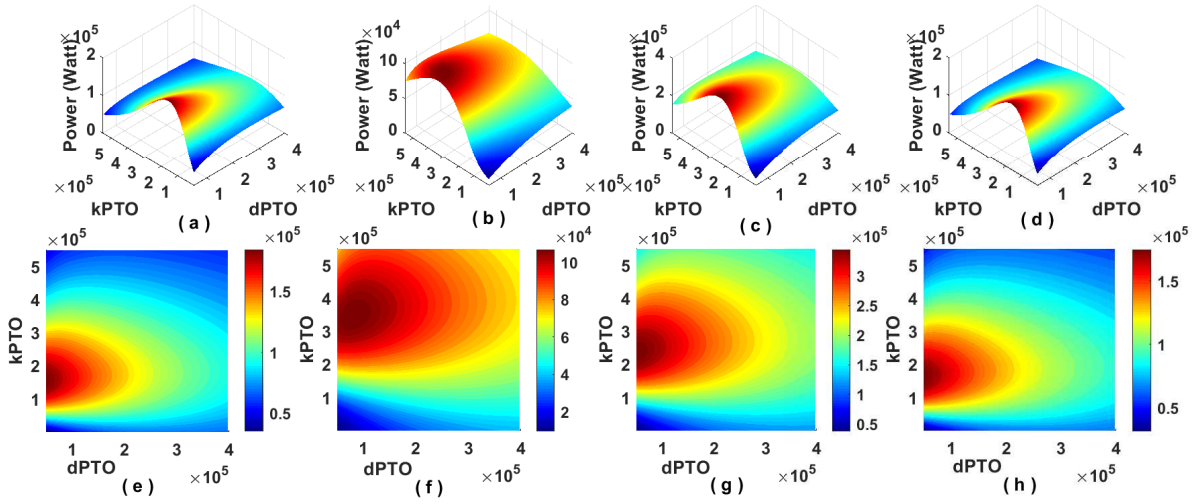


Figure 8: PTOs settings power landscape analysis of four real wave scenarios (Adelaide(a,e), Sydney(b,f), Tasmania (c,g) and Perth (d,h)) for one buoy layout. We assume the most straightforward experiment of PTOs settings with the same value for all 50 wave frequencies. The spring-damping PTO configuration step size is 2500. Note that the real PTOs configurations search space is multi-modal and can be assigned by different values per each wave frequency.

can see that this simplified search space of just one buoy PTOs is multi-modal and complex to search¹. It is also of note that, even in this constrained search environment, there is a 3-fold improvement in extracted energy compared to previous studies [12, 6].

Moreover, to provide an alternative visualization of this experiment, a 4D power landscape is plotted. Figure 10 presents a trade-off of damping ($dPTO$), spring ($kPTO$), wave frequency and absorbed power. We can see that a specific range of frequencies with tuned values of PTO settings can produce more power. Note however the figure is plotted for one fixed buoy without the complex details of hydrodynamic interactions between buoys in the wave farm. A-priori, it is expected that introducing more buoys will produce interactions that will increase the complexity of this landscape further.

The optimisation process of one buoy PTOs based on the 50 wave frequencies by SLPSO can be observed in Figure 11. The PTO values fluctuate several times for each wave frequency and finally, converge to particular values.

6.1.2 Position analysis

For evaluating the position sensitivity of the best-found 16-buoy arrangement in four real wave models, a practical experiment is done. In the first step, we perturb each generator's position by a random variable with a normal distribution ($\mu = (x_i, y_i)$ and $\sigma = 1m$) 100 times. Secondly, we perturb all buoys position by this strategy. Figure 12 demonstrates the results of both perturbation experiments and the best 16-buoy layout power. We can see that this practical analysis is able to improve the total power output of Adelaide wave site by 0.04%. This minor modification

¹Because this diagram is a low-dimensional projection from a higher-dimensional landscape it can't be automatically assumed that the higher-dimensional landscape for PTO optimisation at least, is also multi-modal. Note that previous work has shown that the buoy-positioning landscape is multi-modal, but exploring the multi-modality or otherwise of the entire higher-dimensional search landscape for PTO settings is future work.

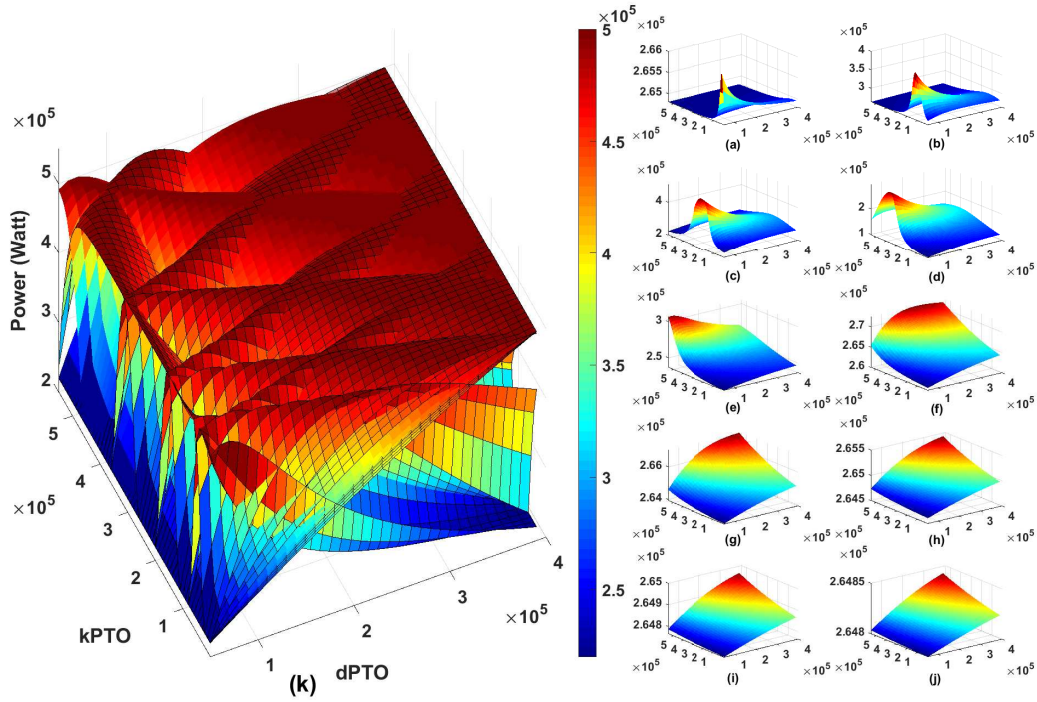


Figure 9: The simplified power landscape of one buoy where PTO parameters are evaluated in ten sequential five-wave frequency groups. Figure (a) demonstrates the PTO (damping-spring parameters) power landscape of one buoy when we assume k and d parameters for f_1, f_2, \dots, f_5 are the same and other 45 wave frequencies are set by the predefined value ($dPTO = 97412, kPTO = 407510$). Other figures follow the same pattern for instance Figure (b) represents the performance of a simple grid search ($Step = 10000$) for plotting the power landscape of f_6, f_7, \dots, f_{10} of tuned PTO parameters. In the left side, Figure (k) shows a normalized overlapping of the surfaces of all ten landscapes in one graph for depicting the complexity level of the search space.

reveals that the proposed optimisation method (HCCA) can converge to a, locally, near-optimal configuration within the limited computational budget appropriately (in terms of position optimisation).

Moreover, for the other three wave scenarios (Sydney, Tasmania, and Perth), the position analysis experiments cannot find a better configuration than the HCCA optimisation results. The perturbation loss, respectively, for the best 16-buoy layouts power in Sydney, Tasmania and Perth wave farm are 0.67%, 0.49% and 0.12% on average. According to the results, the power outputs for the best-found layouts are relatively insensitive to small perturbations in buoy position – this is a good outcome in that small errors in buoy placement in a real environment are unlikely to have a major impact on power output.

6.2 optimisation Experiments

In this part, we summarize the experimental results from optimizing the layout and PTO parameters from 4-buoy arrays and then 16-buoy arrays. The 16-buoy experiments are expected to be more challenging due to the larger number of parameters and a much larger number of buoy interactions.

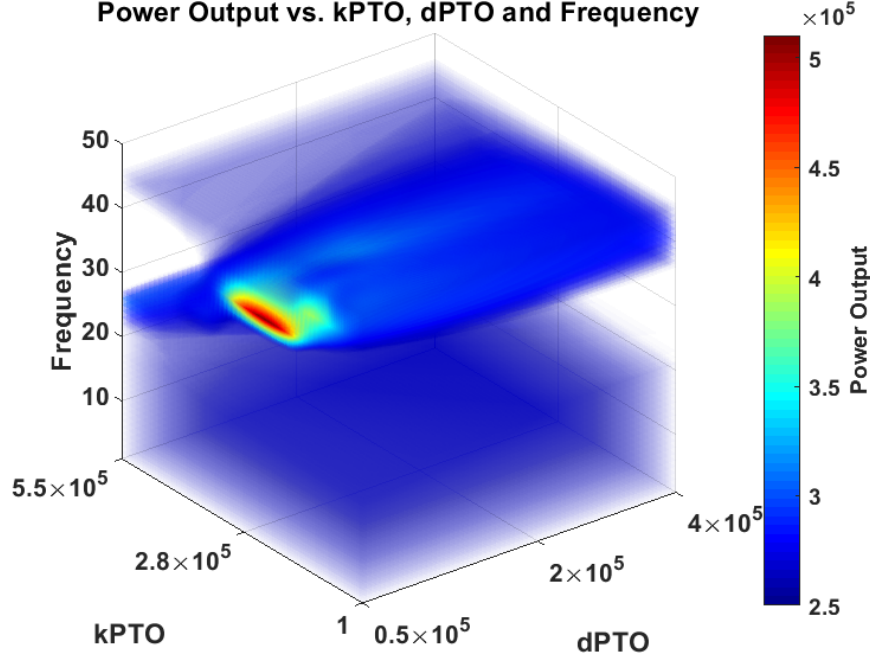
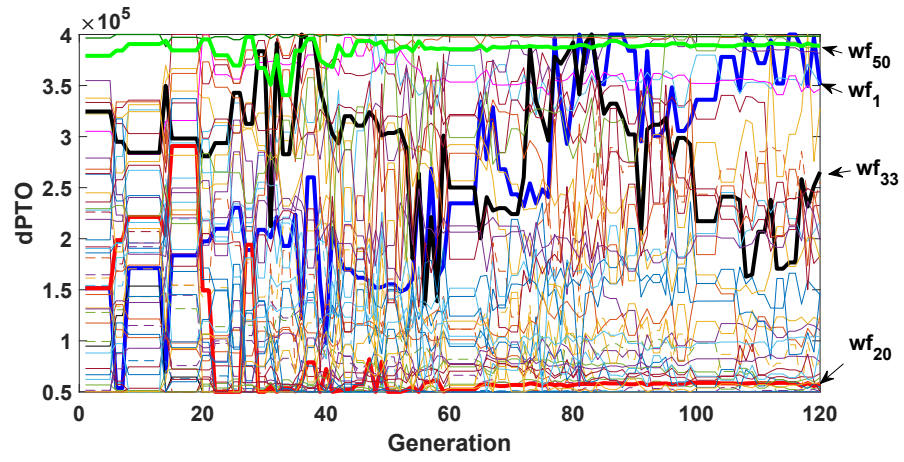


Figure 10: A 4D view PTO power landscape for one buoy in the Perth wave model.

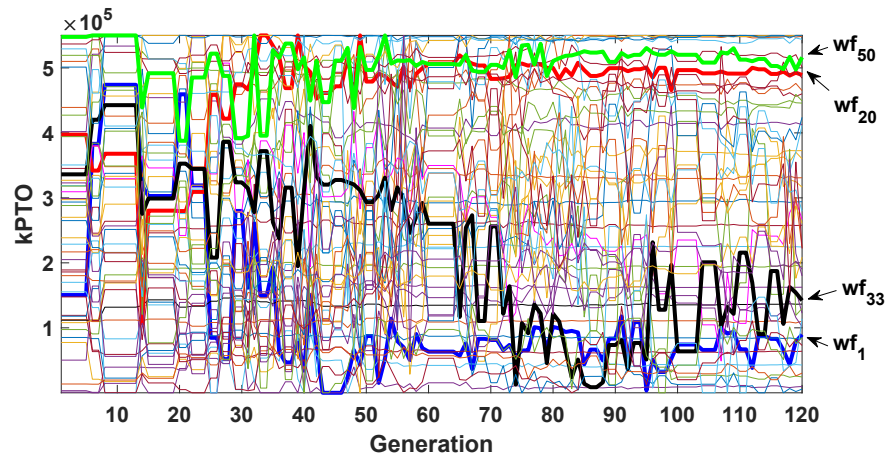
6.2.1 4-buoy layout results

In the experiments on 4-buoy layouts (medium-scale optimisation problem), 15 representative meta-heuristic algorithms are compared with the HCCA including five well-know EAs plus a new adaptive version of GWO, six cooperative EAs and two-hybrid heuristic approaches in four real wave scenarios. The parameter settings for these meta-heuristic variants are summarized in Table 1. The termination condition of each method is reached when three days are exhausted (with 12 cores in parallel). Figure 14 presents the box-and-whiskers plot for the best-found 4-buoy configurations which produce the maximum power output for each run for 16 search heuristics for four real wave models. It can be seen that the performance of cooperative co-evolution strategies (CCOS, SLPSO_{II} and SaNSDE_{II}) and the new hybrid method are considerably better than other applied meta-heuristic algorithms. The next best performances are exhibited by both SLS-NM and SLS-NM-B; however, the average absorbed power by these methods is less than the CC and HCCA approaches by 25%.

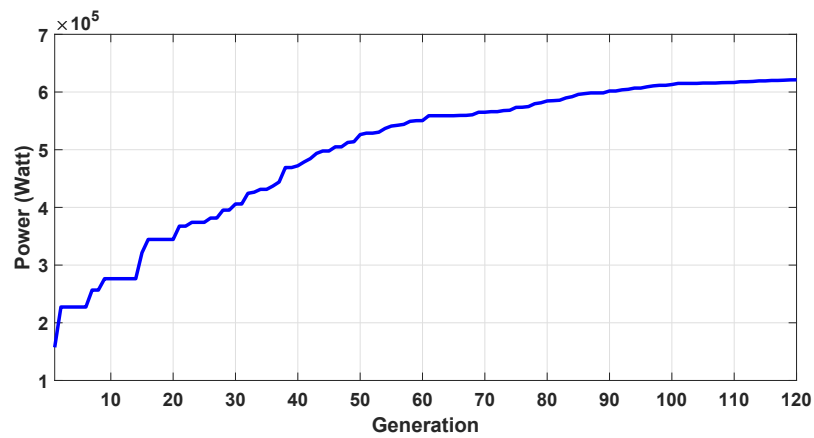
Looking more closely at Table 6, we can observe the highest absorbed power of 4-buoy layouts are found by SLPSO_{II}, CCOS and HCCA, respectively. These optimisation results are closely followed by the SaNSDE_{II} algorithm. These competitive performances are supported by the statistical test results, ranked using the non-parametric Friedman test, shown in Table 4. It is noteworthy to note that among the five optimisation methods in the all-at-once strategy, the GWO and AGWO performances are substantially better than others.



(a)



(b)



(c)

Figure 11: Damping-Spring (dPTO (a) and kPTO (b)) optimisation of one buoy by SLPSO for each wave frequency (f_1, f_2, \dots, f_{50}). The optimisation process of some chosen wave frequencies lines are marked in bold to highlight their trajectories.

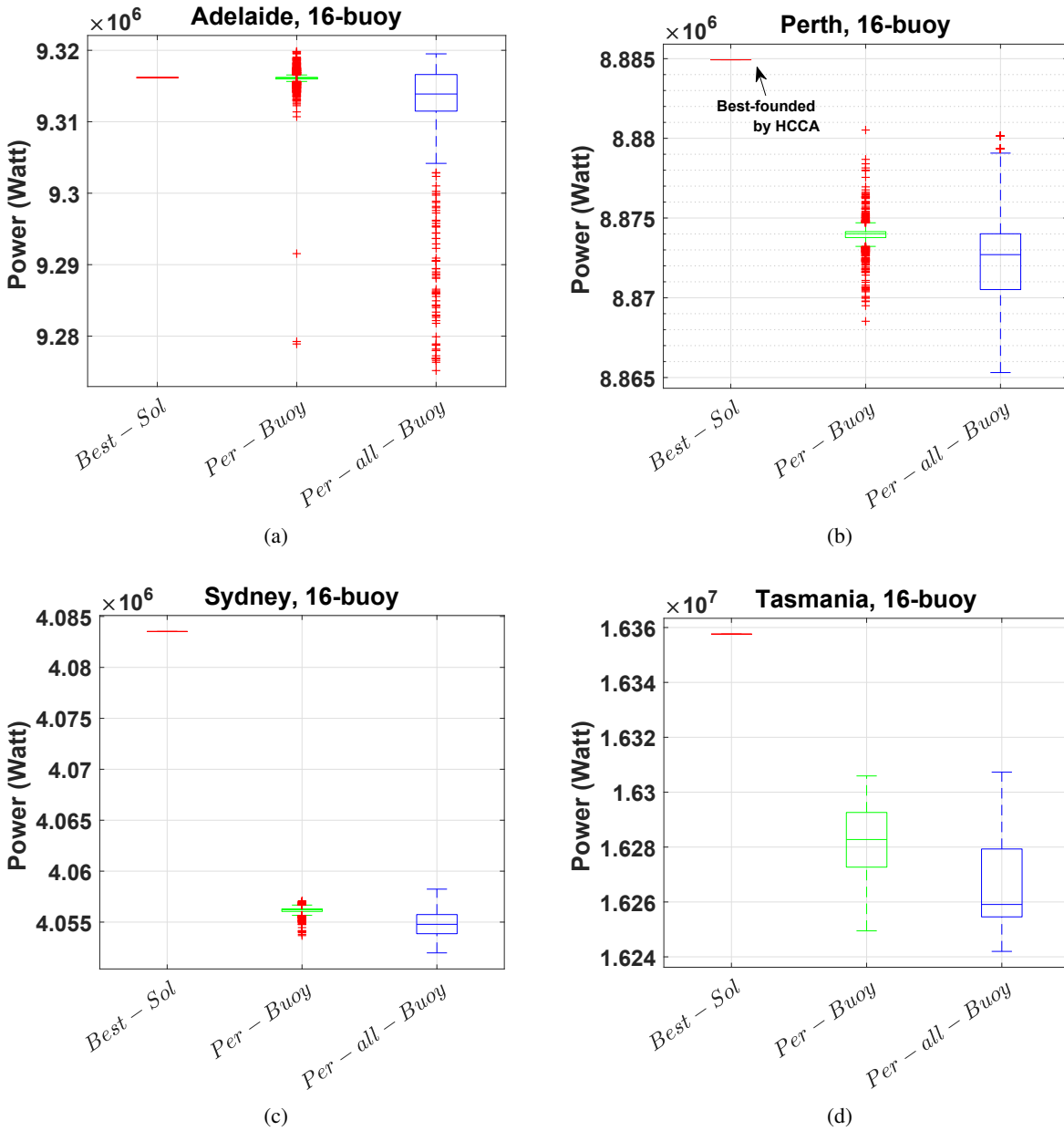


Figure 12: The position perturbation experimental results 16-buoy in 4 real wave models per each buoy and all buoys.

Viewing the convergence curves (Figure 15) from this experiment (4-buoy) in four real wave models, it is clear that the HCCA framework converges faster for the 4-buoy layout than other search methods. In fact, HCCA improves beyond the power outputs achieved by other methods when it has consumed just 20% of its 3-day computational budget.

6.2.2 16-buoy layout results

As evaluating one 16-buoy layout is ten times more expensive than a 4-buoy layout, optimizing such large wave farms is a challenging problem. According to the statistical results of Table 5, we see that the average 16-buoy layouts power output which are found by HCCA is increased substantially to 80% more than previous research outcomes (SLS-NM-B [6]) in all wave scenarios. Table 4 presents the average rank of all heuristic methods for 16-buoy experiments, that HCCA, SLS-NM-B and SLS-NM have the highest rank, respectively.

The best-found 16-buoy layouts power output for each run of all heuristic methods are plotted as a box plot by Figure 13. Figure 13 shows that HCCA performs much better than other optimisation algorithms, as mentioned before. After SLS-NM and SLS-NM-B, The efficiency of the AGWO-NM, AGWO and GWO are competitive compared with other cooperative and generic EAs. The primary reason is derived from the robust exploitation and exploration capability of GWO for PTO parameter optimisation and having good performance for high-dimensional problems. It is noteworthy that the CC frameworks (CCOS, SLPSO_{II} and SaNSDE_{II}) are not shown to be highly effective. This may be because the CC framework is not equipped with the systematic position optimisation mechanism (SLS) used by some of the one-at-a-time placement algorithms.

Figure 16 illustrates the convergence rate of proposed methods experiments during the three-day runtime budget. It is observed that in the initial hours, GWO and their modified versions rapidly converge to effective configurations; however, they could not keep this upward trend and converge toward locally optimal settings. HCCA, clearly, has the fastest convergence speed in the four-wave models. It can be observed that SLS-NM-B is able to converge to a reasonable configuration, but that is not comparable to HCCA's achievements because of the low efficiency of Nelder-Mean optimizing the large-scale PTO parameter part of the problem. Another important observation is that the CC approaches seem to suffer from premature convergence. In addition, they also appear to be not fast enough for such expensive optimisation problems which allow just a few thousand full evaluations (3×10^3). The best 16-buoy layouts of the nominated five methods among all heuristics can be shown in Figure 7, including HCCA, CMA-ES, AGWO-NM, SLPSO_{II} and LS-NM in four real wave scenarios. In terms of position optimisation, it is clearly observed that HCCA is able to adjust the position of each generator successfully, which leads to a distinctive pattern of one or more rows, roughly aligned with the norm of the dominant wave direction, for placing the 16 buoys. This pattern is associated with a fast position optimisation mechanism of SLS-NM [6] that plays the role of one component in HCCA. In contrast, the other best layouts are relatively disordered.

Table 4: The average ranking of the proposed methods by non-parametric statistical test (Friedman test).

Rank	4-buoy						16-buoy					
	Perth	Adelaide	Sydney	Tasmania	Rank	Perth	Adelaide	Sydney	Tasmania			
1	CCOS (1.50)	SLPSO (1.33)	CCOS (1.58)	SLPSO (1.00)	1	HCCA (1.00)	HCCA (1.00)	HCCA (1.00)	HCCA (1.00)			
2	SLPSO (1.83)	CCOS (1.66)	SLPSO (1.83)	SanSDE (2.25)	2	SLS-NM-B (2.16)	SLS-NM-B (2.58)	SLS-NM-B (2.33)	SLS-NM-B (2.50)			
3	HCCA (2.83)	SanSDE (3.41)	HCCA (3.00)	HCCA (2.83)	3	SLS-NM (3.16)	SLS-NM (2.66)	AGWO (3.75)	AGWO-NM (3.33)			
4	SanSDE (3.83)	HCCA (3.58)	SanSDE (3.58)	CCOS (4.33)	4	AGWO-NM (4.58)	AGWO-NM (4.66)	SLS-NM (4.33)	SLS-NM (3.58)			
5	SLS-NM-B (5.42)	SLS-NM-B (5.25)	SLS-NM-B (5.58)	SLS-NM-B (5.08)	5	AGWO (4.75)	AGWO (4.75)	AGWO-NM (4.58)	GWO (5.25)			
6	SLS-NM (5.58)	SLS-NM (5.75)	SLS-NM (5.75)	SLS-NM (5.5)	6	GWO (5.41)	GWO (5.33)	GWO (5.16)	AGWO (5.41)			
7	1+IEA-NM (7.25)	1+IEA-NM (7.50)	1+IEA-NM (6.75)	1+IEA-NM (7.00)	7	CCOS (7.00)	CCOS (7.66)	CCOS (7.00)	CCOS (6.91)			
8	AGWO-NM (9.08)	AGWO (8.75)	CMAES-NM (8.50)	CMAES-NM (8.66)	8	SLPSO (8.08)	SLPSO (8.16)	SLPSO (8.00)	SLPSO (8.08)			
9	AGWO (9.33)	AGWO-NM (9.50)	AGWO-NM (9.91)	AGWO-NM (9.00)	9	SanSDE (9.08)	SanSDE (8.50)	SanSDE (8.83)	SanSDE (9.16)			
10	GWO (10.33)	GWO (10.81)	AGWO (9.91)	AGWO (10.58)	10	LS-NM (10.16)	LS-NM (9.91)	LS-NM (10.58)	LS-NM (10.50)			
11	CMAES-NM (10.75)	CMAES-NM (9.83)	GWO (10.08)	GWO (10.75)	11	CMAES-NM (11.66)	CMAES-NM (11.25)	PSO (11.16)	CMAES-NM (11.16)			
12	PSO (11.91)	PSO (11.00)	LS-NM (12.25)	LS-NM (11.25)	12	DE (12.83)	CMA-ES (12.58)	CMA-ES (13.16)	PSO (11.91)			
13	LS-NM (11.91)	LS-NM (12.41)	PSO (12.25)	PSO (12.75)	13	CMA-ES (13.00)	DE (13.33)	CMAES-NM (13.91)	1+IEA-NM (13.66)			
14	DE (14.25)	DE (14.08)	DE (14.16)	DE (14.25)	14	1+IEA-NM (13.41)	PSO (13.58)	1+IEA-NM (14.00)	DE (13.66)			
15	CMA-ES (14.91)	CMA-ES (14.91)	NM (15.33)	CMA-ES (14.91)	15	PSO (13.75)	1+IEA-NM (14.00)	DE (14.08)	CMA-ES (13.83)			
16	NM (15.25)	NM (16.00)	CMA-ES (15.50)	NM (15.83)	16	NM (15.91)	NM (16.00)	NM (14.08)	NM (16.00)			

Perth wave scenario (16-buoy)															
DE	CMA-ES	NM	GWO	AGWO	PSO	CMAES-NM	I+IEA-NM	AGWO-NM	CCOS	SLPSO _{II}	SaNSDE _{II}	LS-NM	SLS-NM	SLS-NM-B	HCCA
Max	1978004	1707140	3869189	4017436	1874697	2205390	1985315	4071870	2926335	2666886	2460983	2316240	4613064	5355093	8884930
Min	1813302	1764271	1393953	2940571	1798449	1527216	1508531	3048410	2395674	2294175	2092220	1887327	3530473	3949997	8000897
Mean	1876041	1855243	1585395	3517185	1830755	1956295	1830649	3608593	2683725	2507576	2279899	2106215	4010725	4497538	8561839
Median	1876824	1847380	1578621	3218468	1830980	1981432	1889295	3693526	2706138	2528358	2258676	2078183	4010689	4413129	8571208
STD	46761	57806	91733	428449	21004	172404	81722	312569	145881	115616	106092	146586	320417	481974	229971

Sydney wave scenario (16-buoy)															
DE	CMA-ES	NM	GWO	AGWO	PSO	CMAES-NM	I+IEA-NM	AGWO-NM	CCOS	SLPSO _{II}	SaNSDE _{II}	LS-NM	SLS-NM	SLS-NM-B	HCCA
Max	1288869	1290891	1285570	2160341	1345119	1359025	1334937	2427610	1808910	1617776	1573388	1476492	2266424	2441157	4170868
Min	1218526	1222920	1210160	1643183	1290986	1206080	1175279	1938793	1578082	1500364	1436004	1228500	1779821	1983922	4011595
Mean	1250086	1261968	124989	1961163	1320898	1259204	1254215	2101718	1719665	1552703	1499720	1374478	2089419	2345455	4075718
Median	1249281	1261820	1249830	1965235	1326489	1234540	1244844	2116880	1743946	1538400	1487439	1389960	2136654	2381567	4079520
STD	18793	18397	22330	149244	14393	53006	52187	150286	78724	42453	45235	69691	158182	118228	61356

Tasmania wave scenario (16-buoy)															
DE	CMA-ES	NM	GWO	AGWO	PSO	CMAES-NM	I+IEA-NM	AGWO-NM	CCOS	SLPSO _{II}	SaNSDE _{II}	LS-NM	SLS-NM	SLS-NM-B	HCCA
Max	2073818	2066628	1841800	4055518	4198980	2013721	1996107	4331090	2890630	2724026	2600827	2353122	5389570	6305950	9470521
Min	1847975	1925787	1442820	2615454	2828922	1852867	1782396	3129079	2027935	2324849	2177553	1998174	3886630	3731321	8482713
Mean	1942373	1980279	1629929	3386471	3475527	1921268	2076939	3588090	2629506	2521642	2417450	2203759	4424488	4400128	9001224
Median	1947228	1976812	1637145	3397133	3385324	1915633	1863392	3521503	2725506	2512711	2476026	2225386	4271271	4233962	9124786
STD	57795	40254	146374	425179	393443	42836	71047	379587	282542	158706	130958	102117	501941	696882	343378

Tasmania wave scenario (16-buoy)															
DE	CMA-ES	NM	GWO	AGWO	PSO	CMAES-NM	I+IEA-NM	AGWO-NM	CCOS	SLPSO _{II}	SaNSDE _{II}	LS-NM	SLS-NM	SLS-NM-B	HCCA
Max	4102931	4010201	3636190	6752582	7117766	4202333	4130826	8143490	5852075	5351325	4874586	4807895	8891329	11771018	16357582
Min	3815606	3505586	3165160	5297795	5982637	4031614	3713873	7093660	5054946	4615768	4331868	3842791	5830263	7054758	15503720
Mean	3889232	3870418	3388250	6344121	6364880	4105837	3915490	7456337	5477239	4970179	4552102	4332727	7549235	8606078	15952780
Median	3860710	3904263	3393264	6411575	6249592	4097199	3896565	7374770	5499668	4978008	4532614	4295434	7733837	8458468	16070584
STD	76482	136384	146906	414505	362093	48965	141545	287090	232319	199092	173880	284993	964014	1279960	341515

Table 5: Performance comparison of various heuristics for the 16-buoy case, based on maximum, median and mean power output layout of the best solution per experiment.

Perth wave scenario (4-buoy)															
DE	CMA-ES	NM	GWO	AGWO	PSO	CMAES-NM	I+IEA-NM	AGWO-NM	CCOS	SLPSO _{IT}	SaNSDE _{IT}	LS-NM	SLS-NM	SLS-NM-B	HCCA
Max	757152	747703	1203583	1301909	1096161	1181345	1547929	1490604	2589217	2583665	2496828	1056778	1955382	2081568	2571781
Min	679514	684384	862094	980777	898365	664390	1213837	952285	2544542	2505748	2340314	748581	1498860	1513747	2369251
Mean	728521	710025	1055699	1165472	993932	1021743	1376987	1207704	2568664	2556791	2410511	954236	1701684	1780217	2462307
Median	729269	709265	1089776	1166276	986457	1092366	1369274	1196508	2572645	2563001	2408779	970925	1677414	1779828	2460435
STD	23057	18345	123361	108562	97251	66499	81722	166147	15795	25069	45826	86612	116545	164896	62600
Sydney wave scenario (4-buoy)															
DE	CMA-ES	NM	GWO	AGWO	PSO	CMAES-NM	I+IEA-NM	AGWO-NM	CCOS	SLPSO _{IT}	SaNSDE _{IT}	LS-NM	SLS-NM	SLS-NM-B	HCCA
Max	473972	434564	462284	760479	696357	802578	928381	787006	1268449	1272316	1252661	672968	995424	1017464	1262763
Min	434121	406658	352144	616066	542108	692273	768977	620102	1251253	1246321	1182527	493190	785335	847721	1198794
Mean	450864	419080	404325	686588	689951	730352	835518	681253	1260117	1259924	1205699	595972	910660	933515	1228633
Median	453002	416235	409289	683622	601032	726847	819626	679740	1261359	1260302	1200709	604652	933633	911955	1225774
STD	12739	8043	34621	44746	45143	29601	49786	44509	5192	7322	18938	61123	62389	58217	27489
Adelaide wave scenario (4-buoy)															
DE	CMA-ES	NM	GWO	AGWO	PSO	CMAES-NM	I+IEA-NM	AGWO-NM	CCOS	SLPSO _{IT}	SaNSDE _{IT}	LS-NM	SLS-NM	SLS-NM-B	HCCA
Max	828677	764148	722935	1383420	1217127	1147835	1497037	1439554	2720283	2732298	2679951	1161869	2036738	2205885	2711811
Min	706780	730629	520054	984928	1150197	1058355	1215677	978806	2652191	2657184	2514665	903350	1530568	1576432	2303003
Mean	784906	749347	629736	1218747	1088023	1147835	1403663	1211560	2692888	2699379	2603358	1001791	1724642	1818722	2541981
Median	786566	751533	635767	1103790	1098536	1151581	1436140	1193950	2700573	2699965	2617516	970319	1714104	1844716	2574643
STD	33305	11744	78249	123038	72345	55729	80538	157434	21741	23531	56901	82646	156221	178678	124799
Tasmania wave scenario (4-buoy)															
DE	CMA-ES	NM	GWO	AGWO	PSO	CMAES-NM	I+IEA-NM	AGWO-NM	CCOS	SLPSO _{IT}	SaNSDE _{IT}	LS-NM	SLS-NM	SLS-NM-B	HCCA
Max	1520332	1514709	1470010	2274781	2069514	2369299	3221716	2533510	3775336	4808902	4596171	2454579	3842230	3991016	4691217
Min	1411485	1383235	1125670	1963594	1564277	2122243	2612539	2098842	3312687	4743330	4511478	1875692	3028176	3104568	4314911
Mean	1472476	1426742	1272643	2173009	1834935	2369299	2863883	2310503	4786660	4786660	4557535	2094040	3427671	3494835	4512121
Median	1473481	1430254	1236877	2098971	1838107	2398747	2864481	2362061	3836696	4792621	4563350	2040533	3357045	3450918	4507503
STD	46831	37946	104560	111927	89905	100318	185941	147406	351782	20583	33529	185895	271382	299053	95361

Table 6: Performance comparison of various heuristics for the 4-buoy case, based on maximum, median and mean power output layout of the best solution per experiment.

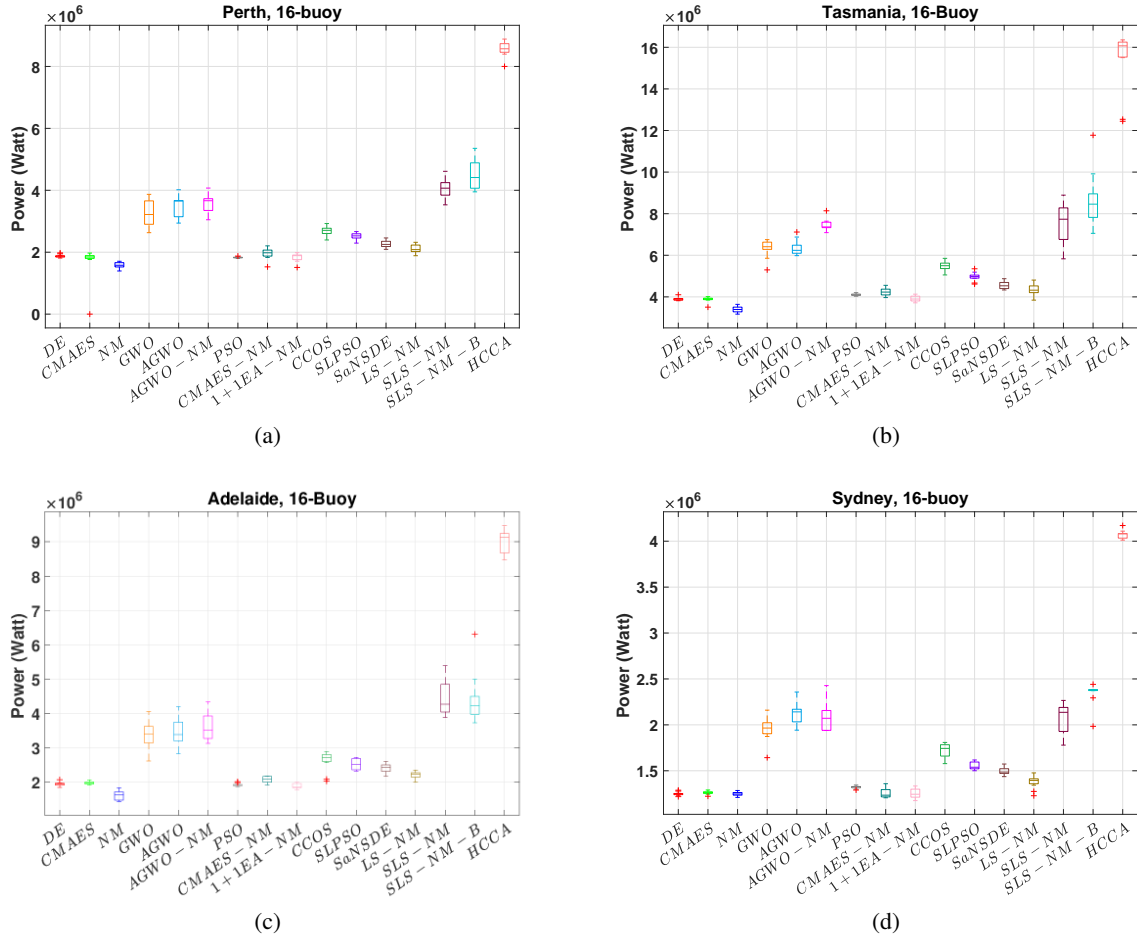


Figure 13: The comparison of the proposed algorithms’ performance for 16-buoy layouts in four real wave model. The optimisation results present the best solution per experiment. (10 independent runs per each method)

7 Conclusions

Optimising a combination of positions and Power Take-off parameters of a wave farm with a large generator number creates a computationally expensive, multi-modal, large-scale and complicated optimisation problem. These challenges are the foremost motivation for discovering faster and smarter optimisation techniques. In this article, we propose a new hybrid cooperative co-evolution method (HCCA) which is composed of a fast strategy for optimising the WEC positions and an effective cooperative strategy (three optimisers) for tuning the PTOs configurations in four real wave scenarios. Moreover, we propose a new adaptive mechanism for improving GWO and the idea is evaluated using ten variants of chaotic maps. To systematically compare the performance of the new search frameworks, we discuss and apply 15 state-of-the-art evolutionary, swarm, alternating (cooperative) and hybrid optimisation algorithms. According to the experimental results, HCCA is able to out-perform other heuristics search methods in terms of convergence speed (5 times faster than the best previous algorithm) and the quality of layouts (80% improvement of the sustained energy output in 16-buoy experiments). In the future, we would like to combine HCCA with a deep

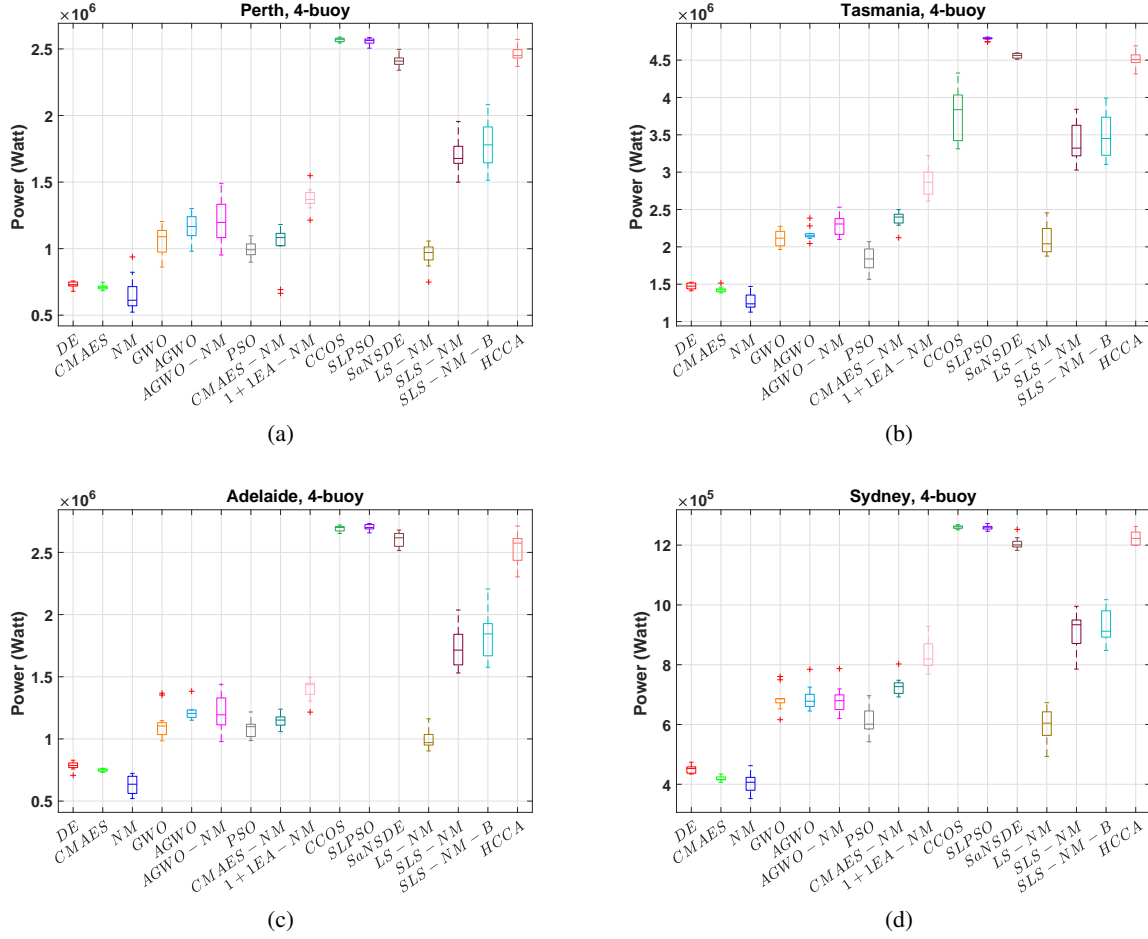


Figure 14: The comparison of the proposed algorithms' performance for 4-buoy layouts in four real wave models. The optimisation results present the best solution per experiment. (10 independent runs per each method)

neuro-surrogate model which is trained using a minimum number of samples for speeding up the evaluation time of the large wave farm. The neuro-surrogate will aim to estimate the total power output based on the wave scenario's characteristics.

Algorithm 3 Backtracking optimisation Algorithm (BOA)

```

1: procedure BOA ( $\mathbb{S}, \mathbb{A}$ )
2: Initialization
3:  $energy = ([E_1, E_2, \dots, E_N]) = Eval(\mathbb{S})$ 
4:  $N_w = round(N/4)$ 
5:  $\langle WIndex \rangle = FindWorst(energy, N_w)$ 
6: for  $i$  in  $[1, \dots, N_w]$  do
7:   Position optimisation
8:    $(\mathbb{S}_{WIndex(i)}^{Position}, energy_{WIndex(i)}) = Nelder-Mead(\mathbb{S}_{WIndex(i)}^{Position})$ 
9: end for
10: PTO global optimisation
11:  $(\mathbb{S}_{PTOs}, energy) = optimise(\mathbb{S}_{PTOs}, \mathbb{A}_{BestIndex})$ 
12: return  $\mathbb{S}, energy$ 
13: end procedure

```

\triangleright Evaluate layout
 \triangleright Buoy number need to be improved
 \triangleright Find worst buoys power
 \triangleright Final Layout

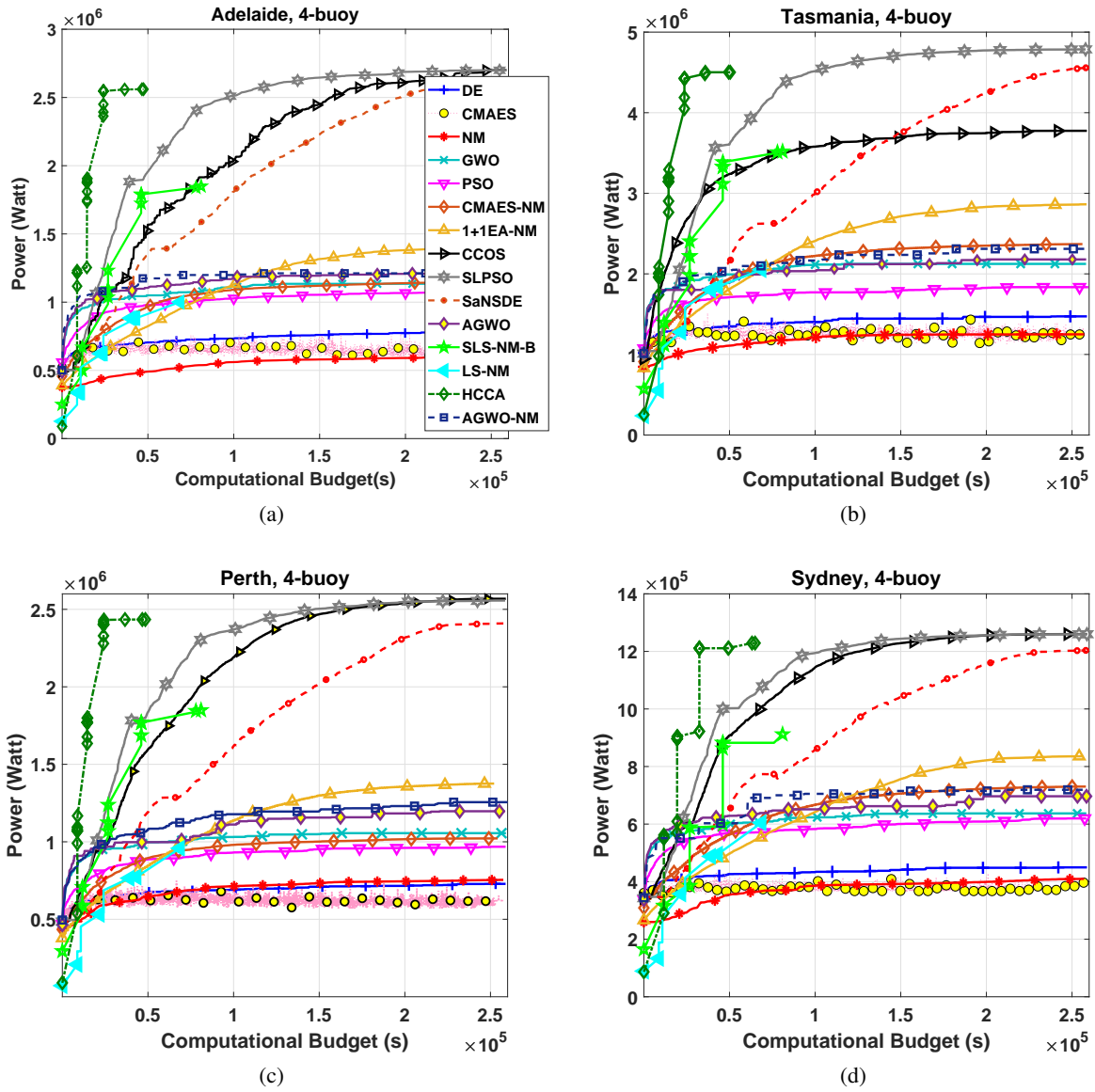


Figure 15: Comparison of algorithms' effectiveness and convergence rate for 4-buoy layouts in four real wave scenarios.

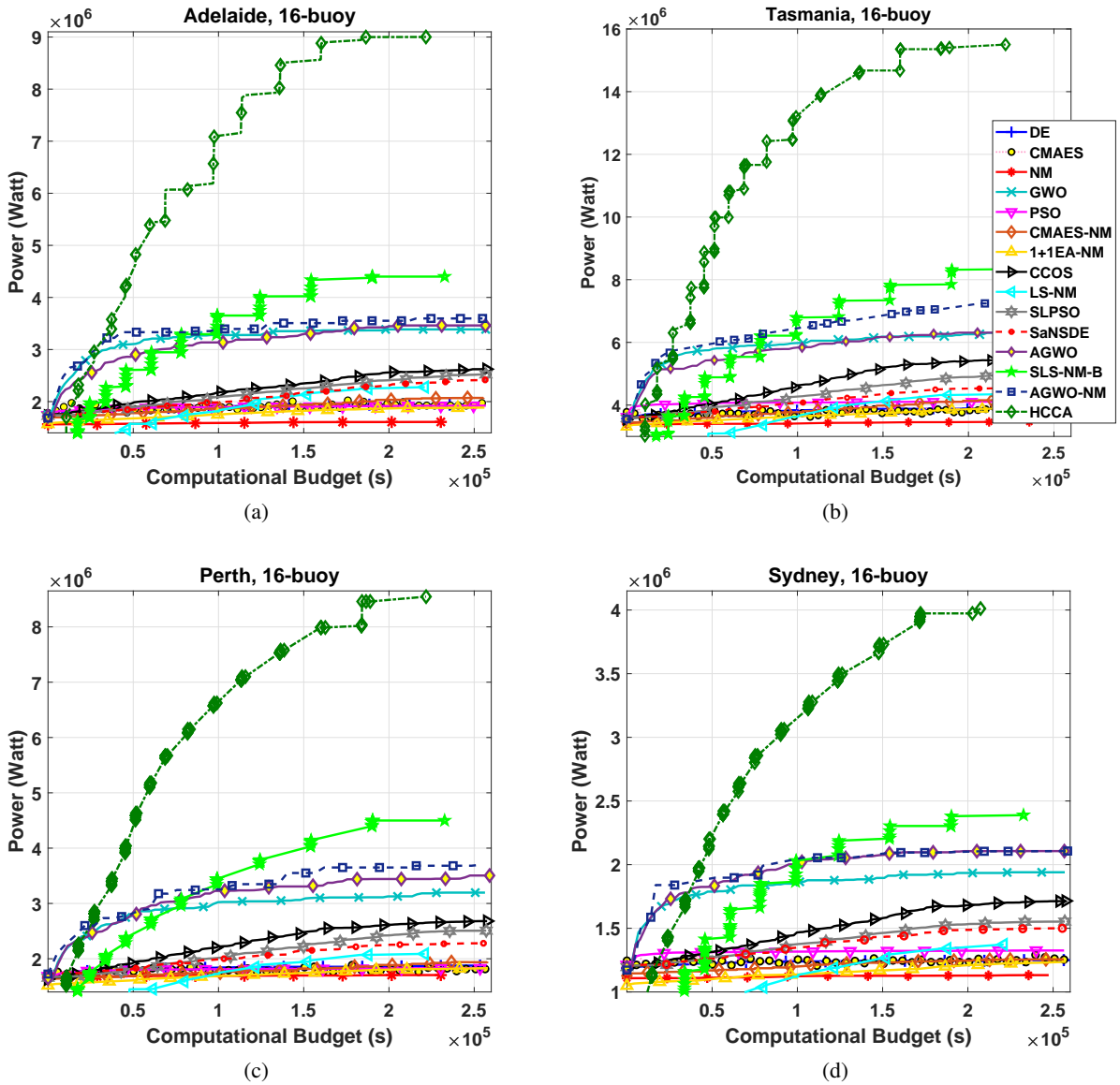


Figure 16: Comparison of algorithms' performance and convergence rate for 16-buoy layouts in four real wave scenarios.

References

- [1] Michael Liebreich. Bloomberg new energy finance summit. *London: Bloomberg New Energy Finance*, 2013.
- [2] B Drew, A R Plummer, and M N Sahinkaya. A review of wave energy converter technology. *Proceedings of the Institution of Mechanical Engineers, Part A: Journal of Power and Energy*, 223(8):887–902, 2009.
- [3] Yan Yaobao. Principle and device of the ocean wave energy conversion generation. *Shanghai Scientific and Technical Publishers*, 1(1):21–24, 2013.
- [4] Laurence D Mann. Application of ocean observations & analysis: The ceto wave energy project. In *Operational Oceanography in the 21st Century*, pages 721–729. Springer, 2011.
- [5] L. D. Mann, A. R. Burns, , and M. E. Ottaviano. Ceto, a carbon free wave power energy provider of the future. In *the 7th European Wave and Tidal Energy Conference (EWTEC)*, 2007.
- [6] Mehdi Neshat, Bradley Alexander, Nataliia Y. Sergiienko, and Markus Wagner. A hybrid evolutionary algorithm framework for optimising power take off and placements of wave energy converters. In *Proceedings of the Genetic and Evolutionary Computation Conference, GECCO '19*, pages 1293–1301, New York, NY, USA, 2019. ACM.
- [7] BFM Child and Vengatesan Venugopal. Optimal configurations of wave energy device arrays. *Ocean Engineering*, 37(16):1402–1417, 2010.
- [8] Pau Mercadé Ruiz, Vincenzo Nava, Mathew BR Topper, Pablo Ruiz Minguela, Francesco Ferri, and Jens Peter Kofoed. Layout optimisation of wave energy converter arrays. *Energies*, 10(9):1262, 2017.
- [9] Nikolaus Hansen. The cma evolution strategy: a comparing review. *Towards a new evolutionary computation*, pages 75–102, 2006.
- [10] KN Krishnanand and Debasish Ghose. Glowworm swarm optimization for simultaneous capture of multiple local optima of multimodal functions. *Swarm Intelligence*, 3(2):87–124, 2009.
- [11] Junhua Wu, Slava Shekh, Nataliia Y Sergiienko, Benjamin S Cazzolato, Boyin Ding, Frank Neumann, and Markus Wagner. Fast and effective optimisation of arrays of submerged wave energy converters. In *Genetic and Evolutionary Computation Conference (GECCO)*, pages 1045–1052. ACM, 2016.
- [12] Mehdi Neshat, Bradley Alexander, Markus Wagner, and Yuanzhong Xia. A detailed comparison of meta-heuristic methods for optimising wave energy converter placements. In *Genetic and Evolutionary Computation Conference (GECCO)*, pages 1318–1325. ACM, 2018.
- [13] Mehdi Neshat, Bradley Alexander, Nataliia Y. Sergiienko, and Markus Wagner. A new insight into the position optimization of wave energy converters by a hybrid local search. *CoRR*, abs/1904.09599:1–23, 2019.
- [14] Mehdi Neshat, Ehsan Abbasnejad, Qinfeng Shi, Bradley Alexander, and Markus Wagner. Adaptive neuro-surrogate-based optimisation method for wave energy converters placement optimisation. *arXiv preprint arXiv:1907.03076*, 2019.

- [15] Johannes Falnes. *Ocean waves and oscillating systems: linear interactions including wave-energy extraction*. Cambridge University Press, 2002.
- [16] Boyin Ding, Benjamin S Cazzolato, Maziar Arjomandi, Peter Hardy, and Bruce Mills. Sea-state based maximum power point tracking damping control of a fully submerged oscillating buoy. *Ocean Engineering*, 126:299–312, 2016.
- [17] Ossama Abdelkhalik and Shadi Darani. Optimization of nonlinear wave energy converters. *Ocean Engineering*, 162:187–195, 2018.
- [18] Marianna Giassi and Malin Göteman. Layout design of wave energy parks by a genetic algorithm. *Ocean Engineering*, 154:252–261, 2018.
- [19] S Ribeiro e Silva, RPF Gomes, and AFO Falcao. Hydrodynamic optimization of the ugen: Wave energy converter with u-shaped interior oscillating water column. *International Journal of Marine Energy*, 15:112–126, 2016.
- [20] Michael JD Powell. A direct search optimization method that models the objective and constraint functions by linear interpolation. In *Advances in optimization and numerical analysis*, pages 51–67. Springer, 1994.
- [21] Australian wave energy atlas, 2016.
- [22] Charles L Bretschneider. The generation and decay of wind waves in deep water. *Eos, Transactions American Geophysical Union*, 33(3):381–389, 1952.
- [23] JT Scruggs, SM Lattanzio, AA Taflanidis, and IL Cassidy. Optimal causal control of a wave energy converter in a random sea. *Applied Ocean Research*, 42:1–15, 2013.
- [24] GX Wu. Radiation and diffraction by a submerged sphere advancing in water waves of finite depth. In *Proc. of the Royal Society of London A: Mathematical, Physical and Engineering Sciences*, volume 448, pages 29–54. The Royal Society, 1995.
- [25] James C Bezdek and Richard J Hathaway. Convergence of alternating optimization. *Neural, Parallel & Scientific Computations*, 11(4):351–368, 2003.
- [26] Rainer Storn and Kenneth Price. Differential evolution—a simple and efficient heuristic for global optimization over continuous spaces. *Journal of global optimization*, 11(4):341–359, 1997.
- [27] Russell Eberhart and James Kennedy. A new optimizer using particle swarm theory. In *Symposium on Micro Machine and Human Science (MHS)*, pages 39–43. IEEE, 1995.
- [28] Seyedali Mirjalili, Seyed Mohammad Mirjalili, and Andrew Lewis. Grey wolf optimizer. *Advances in engineering software*, 69:46–61, 2014.
- [29] Jeffrey C Lagarias, James A Reeds, Margaret H Wright, and Paul E Wright. Convergence properties of the nelder–mead simplex method in low dimensions. *SIAM Journal on optimization*, 9(1):112–147, 1998.
- [30] Agoston E Eiben, Zbigniew Michalewicz, Marc Schoenauer, and James E Smith. Parameter control in evolutionary algorithms. In *Parameter setting in evolutionary algorithms*, pages 19–46. Springer, 2007.

- [31] Yuan Sun, Michael Kirley, and Xiaodong Li. Cooperative co-evolution with online optimizer selection for large-scale optimization. In *Proceedings of the Genetic and Evolutionary Computation Conference*, pages 1079–1086. ACM, 2018.
- [32] Nitin Mittal, Urvinder Singh, and Balwinder Singh Sohi. Modified grey wolf optimizer for global engineering optimization. *Applied Computational Intelligence and Soft Computing*, 2016:8, 2016.
- [33] Wen Long, Ximing Liang, Shaohong Cai, Jianjun Jiao, and Wenzhuan Zhang. A modified augmented lagrangian with improved grey wolf optimization to constrained optimization problems. *Neural Computing and Applications*, 28(1):421–438, 2017.
- [34] Akash Saxena, Rajesh Kumar, and Swagatam Das. β -chaotic map enabled grey wolf optimizer. *Applied Soft Computing*, 75:84–105, 2019.
- [35] Gaganpreet Kaur and Sankalop Arora. Chaotic whale optimization algorithm. *Journal of Computational Design and Engineering*, 5(3):275–284, 2018.
- [36] Shahrzad Saremi, Seyedali Mirjalili, and Andrew Lewis. Biogeography-based optimisation with chaos. *Neural Computing and Applications*, 25(5):1077–1097, 2014.
- [37] Gai-Ge Wang, Lihong Guo, Amir H Gandomi, Guo-Sheng Hao, and Heqi Wang. Chaotic krill herd algorithm. *Information Sciences*, 274:17–34, 2014.
- [38] Xiangtao Li and Minghao Yin. Modified cuckoo search algorithm with self adaptive parameter method. *Information Sciences*, 298:80–97, 2015.
- [39] Yuan Sun, Michael Kirley, and Saman K Halgamuge. A recursive decomposition method for large scale continuous optimization. *IEEE Transactions on Evolutionary Computation*, 22(5):647–661, 2017.
- [40] Ran Cheng and Yaochu Jin. A social learning particle swarm optimization algorithm for scalable optimization. *Information Sciences*, 291:43–60, 2015.
- [41] Zhenyu Yang, Ke Tang, and Xin Yao. Self-adaptive differential evolution with neighborhood search. In *2008 IEEE Congress on Evolutionary Computation (IEEE World Congress on Computational Intelligence)*, pages 1110–1116. IEEE, 2008.
- [42] Lixing Han and Michael Neumann. Effect of dimensionality on the nelder–mead simplex method. *Optimization Methods and Software*, 21(1):1–16, 2006.
- [43] Zhenyu Yang, Ke Tang, and Xin Yao. Large scale evolutionary optimization using cooperative coevolution. *Information Sciences*, 178(15):2985–2999, 2008.
- [44] Bruno Borgarino, Aurélien Babarit, and Pierre Ferrant. Impact of wave interactions effects on energy absorption in large arrays of wave energy converters. *Ocean Engineering*, 41:79–88, 2012.

- [45] Mohammad Nabi Omidvar, Ming Yang, Yi Mei, Xiaodong Li, and Xin Yao. Dg2: A faster and more accurate differential grouping for large-scale black-box optimization. *IEEE Transactions on Evolutionary Computation*, 21(6):929–942, 2017.